ABSTRACT

Title of Thesis: MODELING URBAN FLOODING IN THE TIBER BRANCH WATERSHED, ELLICOTT CITY, MARYLAND, USING PCSWMM

Cadijah J Walcott, Master of Science, 2020

Thesis directed by: Professor Kaye Brubaker, Department of Civil and Environmental Engineering

Urban flooding — due to land cover change, inadequate drainage networks, and increased precipitation — exacerbates communities' economic and social vulnerabilities. A detailed watershed model can help communities identify weak portions of the drainage network and design resolutions. This research details the development of a comprehensive model of the Tiber Branch Watershed in Ellicott City, Maryland, to reproduce observed depth in the Hudson Branch tributary using PCSWMM (a commercial version of the U.S. Environmental Protection Agency's Storm Water Management Model). The 2,434.8-acre watershed comprises 8,821 PCSWMM objects, which were estimated from various raster and vector datasets. Without calibration, the model generally captures the timing and shape of the stage hydrographs but is less successful in simulating event magnitude and receives a R^2 of 0.65 and SE/SY of 0.67 for the 43 selected events, collectively. Ultimately, model evaluation was not completed due to a lack of representative rainfall within the watershed.

MODELING URBAN FLOODING IN THE TIBER BRANCH WATERSHED, ELLICOTT CITY, MARYLAND, USING PCSWMM

by

Cadijah J Walcott

Thesis submitted to the Faculty of the Graduate School of the
University of Maryland, College Park, in partial fulfillment
of the requirements for the degree of
Master of Science
2020

Advisory Committee:
Professor Kaye Brubaker, Chair
Professor Richard McCuen
Professor Allison Reilly

Acknowledgements

I wish to express my deepest gratitude to my incredible advisor, Dr. Brubaker for her unwavering support and guidance. Thank you for your time and patience during our meetings for the past two years and the educational and professional support that has my furthered my engineering abilities in the water resources field.

I would like to thank Howard County's Storm Water Management Division for their mentoring over the summer and the various datasets I was provided that assisted in creating my model. Thank you to Maryland's State Highway Administration for providing as-builts for portions of the stormwater network along the state highways.

Thank you, thank you, thank you to my family and friends, especially my momma and partner Benjamin for keeping me sane during trying times and the continuous encouragement. Thank you, momma, for assisting me with my thesis, words cannot express how grateful I am to have the most supportive momma. Thank you, Ben, for bringing a smile to my face every day, suggesting outdoor time, and picking up household duties during my busiest times.

I am truly grateful for the support I have received during my master's program. Thank you.

Table of Contents

List of Tables

List of Figures

List of Abbreviations

Abbreviation	Full Description
CHI	Computational Hydraulics International
CN	Curve Number
DEM	Digital Elevation Model
DFIRM	Digital Flood Insurance Rate Maps
EPA	Environmental Protection Agency
FEMA	Federal Emergency Management Agency
FIRM	Flood Insurance Rate Maps
GIS	Geographic Information System
GOF	Goodness of Fit
HEC-RAS	Hydrologic Engineering Center's River Analysis System
HSG	Hydrologic Soil Group
ISE	Integral Squared Error
LID	Low Impact Development
MRC	Manning's roughness coefficient
NFIP	National Flood Insurance Program
NHD	USGS National Hydrography Datasets
NOAA	National Oceanic and Atmospheric Administration
NRCS	Natural Resources Conservation Service
NWS	National Weather Service
PCSWMM	Personal Computer Storm Water Management Model
RMSE	Root Mean Square Error
SCS	Soil Conservation Survey
SE	Standard Error of Estimates
SRTC	Sensitivity Based Radio Tuning Calibration
SSURGO	Soil Survey Geographic Database
SWM	Stormwater Management Ponds
SWMM	Storm Water Management Model
SY	Standard Deviation of the Observed Data
TBW	Tiber Branch Watershed
UFAA	Urban Flooding Awareness Act
USACE	United States Army Corps of Engineers
USDA	United States Department of Agriculture
USGCRP	U.S. Global Change Research Program
USGS	United States Geological Survey

Chapter 1. Introduction

The urban population continues to grow, and the community spills out of its boundaries into suburban regions for bigger homes and land, while keeping the city within reach. With urbanization comes the increase in impervious surfaces that do not allow for the infiltration of rainfall, resulting in the immediate commencement of runoff. Climate change projections include more frequent and extreme rain events that are the catalyst for urban flooding. Past data no longer reflect the present or the future, and the nonstationary of the data will call for more frequent rainfall frequency analysis. Stormwater networks in urban areas are typically designed for a 10-25-year storm that was computed using design criteria that did not include climate change projections (NOAA Office for Coastal Management, 2020). The determined return periods may be inaccurate, and what may have been a 25-year storm in the past may not be the same presently. Changes to design criteria will impact a stormwater network's performance with more frequent and intense storms.

1.1 Types of Flooding

Flooding is known as the top disaster in the United States and costs billions to respond to and recover from. There are three main types of floods: riverine (fluvial), coastal, and urban (pluvial). Riverine flooding occurs when a stream exceeds its capacity and overflows its banks. Coastal flooding develops from storm surge, and urban flooding is inland flooding caused by many factors, but most known is the failure of the stormwater network to drain runoff from the surface efficiently. Urban flooding occurs when a rain event overwhelms a drainage system, and excess rainfall uses the

surface as a pathway to the outfall causing flooded roads and buildings. In many cities with combined sewer systems, the overwhelmed system may cause sewer backups into homes and discharge of untreated wastewater to untreated water bodies. Nuisance and flash floods can occur in non-urban areas as well but are still components of urban flooding. Nuisance flooding in an urban setting is generally caused by rainfall that is trapped in deep depressions and ponds with water depth between 1.2 and 3.9 inches, which typically reaches the bottom of a car but is not enough water to move a parked car (Moftakhari, et al., 2018). This type of flooding is not a direct threat to public safety but significantly impacts the ability to do normal daily activities. Over time, nuisance flooding can damage infrastructure and cripple stormwater networks with increasing cost to repair.

Flash floods are large volumes of water that flow quickly while propelling debris along the way. They are very dangerous and generally occur within 6 hours of a heavy rainfall event, motivated by poor infiltration and inundated stormwater systems. Flash floods are a concern for public safety; they may result in loss of life and widespread damage to infrastructure, buildings, and cars. Ellicott City, Maryland made national news in July 2016 for a devastating flash flood that ravaged the old historic town and claimed two lives. The National Weather Service (NWS) estimated that approximately 6 inches of rain fell in less than two hours, corresponding to a 1000-year storm, a very rare event (NWS, 2016). The abundance of rain overwhelmed the stormwater drainage network and caused an abrupt and sharp increase of flow in streams and the Patapsco River. The steep slopes of Old Town coupled with impervious surfaces increased the quantity and flow of runoff on the surface and not in the

subsurface network, leading runoff down Main Street. This flash flood resulted in individuals being trapped in flooded buildings, cars and debris swept away and significant damage to infrastructure. A state of emergency was declared, and the city began to rebuild. Less than two years later, a flash flood warning was issued for Ellicott City. NWS estimated between 6-9 inches of rainfall in 3 hours, another *rare* event that damaged the rebuilding community and claimed another life (NWS, 2018). Howard County was tasked with engineering a solution that reduced runoff from the roads while preserving the historical charm that many love.

1.2 Urban Flooding Challenges

In a study completed on urban flooding, 83% of floodplain and stormwater managers representing the contiguous United States reported experiencing flooding in their community, alluding to urban flooding being a national dilemma (UMD CDR and TAMU CTBS, 2018). Although flooding is the top reported disaster, urban floods are customarily left out of reports as a result of difficulties tracking all floods, small and large. More minor floods do not amount to economic damages that are essential for requesting federal assistance and go unnoticed. Smaller communities are forced to deal with urban flooding on a local level with local funds.

Urban watersheds vary in land use, percent of pervious areas, and slope. The increase in impervious surfaces causes an increase in peak discharge, volume of water in roads and streams, and the frequency of floods a community will experience. Impervious surface causes runoff to rapidly move from overland flow to pipe flow instead of a slower pace in overland flow where infiltration can occur more. Rain falling

on steep slopes has less time to infiltrate into soils, and the steepness will affect the efficiency of inlets' capabilities of intercepting runoff.

The Federal Emergency Management Agency (FEMA) works with over 20,000 communities throughout the United States to develop Flood Insurance Rate Maps (FIRMs) through its Risk Mapping Assessment and Planning (RISK Map) program to identify areas at risk of flooding, particularly riverine flooding (FEMA, 2020). These maps are widely used by stormwater management agencies to mitigate and design measures to protect their communities and by residents to identify if current or future property is in a special hazard flood zone. Although the RISK Map is used to identify areas at risk of flooding, the data used to create maps are outdated and may not represent the current status of an area, leaving the risk of flooding in some vulnerable populations unknown. Additionally, some communities are grappling with inadequate sized and poorly maintained drainage systems which also leads to flooding and deserve to comprehend the influence rain events will have on their capacity to carry out everyday tasks.

Watershed modeling is a useful tool a community can utilize to identify problem areas, design low impact development projects that capture rain where it falls and educate residents on flood risks with little expense. Urban flooding is difficult to predict; however, the use of rainfall-runoff models to simulate various scenarios will provide useful information for reducing flooding through management and design. Watershed modeling for water quantity and flooding issues is a much-needed proactive step to protect the lives, property, and economic wellbeing of a community. The

increase in technology and the availability of diverse datasets have allowed for more comprehensive models to be created and used for management and design purposes.

1.3 Research Goal and Objectives

The purpose of this study is to develop and calibrate a model to accurately estimate runoff in the Tiber Branch Watershed (TBW) in Ellicott City, Maryland. The Environmental Protection Agency's (EPA) Storm Water Management Model (SWMM) software (EPA, 2020) was selected for this research for its capabilities to model urban areas and represent the relationship between overland flow and pipe flow.

The original study objectives were as follows:

1. Produce a SWMM model that represents the overland flow and stormwater network in the TBW.
2. Identify the model's sensitivity to changes in parameters' values.
3. Calibrate and validate the model to reproduce observed data.
4. Identify Low Impact Development (LID) projects that can reduce runoff.

In the course of the work, as further described in this thesis document, it became apparent that developing, calibrating, and validating such a detailed model was a major undertaking and that — despite the wealth of data available — calibration and validation would require information and effort beyond the scope. The objectives were revised to be more realistic, as follows:

1. Produce a SWMM model that represents the overland flow and stormwater network in the TBW.

2. Identify the model's sensitivity to changes in parameters' values.
3. Detail challenges with creating an extensive model for a large urban watershed.
4. Identify data needs for the calibration and validation phases of model development.
5. Provide suggestions for application of the model to investigate the potential of LID to reduce urban flooding in the TBW.

Chapter 2. Literature Review

2.1 Urban Flooding

For this study, urban areas include cities and the surrounding region and range in size from small neighborhoods to large communities. The State of Illinois defines urban flooding in the Urban Flooding Awareness Act (UFAA) as "inundation of property in a built environment, particularly in more densely populated areas, caused by rainfall overwhelming the capacity of drainage system" (IDNR, 2015). Although flooding can occur in undeveloped or agricultural regions, the UFAA emphasizes that urban flooding occurs in highly developed and populated areas with very little open space (in comparison to rural and undeveloped regions), which increases the likelihood of flooding. In addition to overland flooding, urban flooding includes "stormwater enter[ing] buildings through windows, doors, or other openings, water back[ing] up through sewer pipes, showers, toilets, sinks, and floor drains, and seepage through walls and floors" (IDNR, 2015).

Urban flooding is very complex and involves a variety of scenarios that can impact an entire population. The combination of precipitation, rapid changes in land use, and inadequate and deteriorating storm drainage systems induce urban flooding. The *Climate Science Special Report* estimates that climate change will exacerbate the intensity and frequency of precipitation in the future for the United States (USGCRP, 2017). Urban development has decreased the percentage of pervious surfaces and replaced it with buildings, roads, and other impervious surfaces decreasing infiltration capabilities, leading to more surface runoff going to the stormwater drainage systems.

Stormwater drainage systems are outdated, poorly maintained, and may be constructed to convey a 10-25-year storm (NOAA OCM, 2020). Ultimately, communities are unable to efficiently remove precipitation and remain vulnerable to inconvenience, damage, and sometimes loss of life.

2.1.1 Impacts on Communities

Globally, urban land is expected to increase from 3.1% to 8.1% of total land area by 2050, with the city-dwelling portion of population estimated to increase from 51% to 68%, putting more people at risk of being affected by urban flooding (Nowak, 2005; United Nations, 2018). Not only does urban flooding affect public spaces, but it also affects people's most valuable possessions: their homes, cars, and lives. Outcomes from flooding are categorized into direct and indirect impacts. Direct impacts are physical damage (to properties, vehicles, and infrastructure) and death. In contrast, indirect impacts are secondhand repercussions from floods and include loss of income, inaccessibility to transportation, distress, and sickness (Kreibich, et al., 2010). Economical, sociological, and psychological distress are all subsets of indirect impacts of flooding with consequences that worsen vulnerabilities. There is no database for tracking urban flooding in the federal, state, or local government to provide an estimate of the real cost of urban flood direct and indirect impacts (UM CDR and TAMU CTBS, 2018). Occasionally, the NWS reports urban floods with astounding rainfall intensities and damages but misses smaller floods that do not amount to coverage due to smaller monetary damages.

Urban floods can occur at a considerable distance from the FEMA designated floodplains, which are located on the outer banks of streams and rivers. Constituents

with a federally backed mortgage in a participating community are required to purchase insurance from the National Flood Insurance Program (NFIP). NFIP only provides insurance for people within the designated floodplain and does not account for people affected by flooding in urban areas that are not associated with riverine or coastal flooding. The perception of risk is skewed for residents living in highly developed areas far from water bodies since NFIP insurance is not required, and lack of flooding transparency in the real estate industry. Additionally, a flooding event must be a presidentially declared disaster to access FEMA's assistance in forms of human resources, grants, and loans. More often than not, smaller urban floods do not amount to required damages to request federal aid, even if it may devastate a community (UM CDR and TAMU CTBS, 2018).

2.2 Urban Flood Modeling

The basis of stormwater management is to understand how effectively a system can remove precipitation from the surface and in what manner. Due to the complexities of an urban area, modeling flooding in an urban region is more complicated than in rural areas or along stream banks. Urban flooding involves modeling the stormwater drainage system to convey the water entering and leaving the system at any location. Increases in technology have allowed for different modeling techniques to be used to represent the interaction between the pipe system and overland flooding on the surface.

2.2.1 Model Selection

In stormwater management, there are three main types of modeling: hydrologic, hydraulic, and water quality. Hydrologic modeling involves land cover, soil characteristics, and topography of a specific area to estimate runoff hydrographs, which predicts runoff volumes and peak flows (MPCA, 2020a). Hydraulic models assess the channel and conduit behavior of the drainage system by estimating "water surface elevations, energy grade lines, flow rates, velocities, and other flow characteristics" (MPCA, 2020b). Water quality models are used to model pollutants concentrations and movement.

For this study, a model that combined hydrologic and hydraulic modeling was necessary to simulate urban flooding and identify weak portions of a stormwater network. In addition, the software capability criteria included large scale modeling of an urban region, event and continuous modeling, and integration of sociological data for visual assessment. According to the Minnesota Pollution Control Agency (MPCA, 2020a), 17 combined hydrologic/hydraulic software programs are available that meet these criteria. The EPA's SWMM capabilities explicitly met the criteria and it was selected for this study. In a McCormick & Taylor report completed on flood analysis in Ellicott City, Maryland, the Natural Resources Conservation Service's (NRCS) TR-20 and TUFLOW software were utilized to model the July 2016 storm (McCormick & Taylor, 2017). TR-20 generated the hydrologic input for the hydraulic model, TUFLOW. The report only considered portions of the river network and not the entire drainage area flowing to the river. Neither the proprietary TUFLOW software nor the Ellicott City model developed by McCormick & Taylor (2017) with that software was

available for use in this study. SWMM, an open-source combined hydrologic/hydraulic model, removes the additional steps of needing multiple models and allows the extensive modeling of pipe and channel flow for further investigative flood analysis.

2.2.2 Environmental Protection Agency's Stormwater Management Model

The EPA developed and released the open-source software, SWMM, in 1969 with four updates since its inception. Developed as a "dynamic rainfall-runoff simulation model used for a single event or long-term (continuous) simulation of runoff quantity and quality from primarily urban areas" (Rossman & Huber, 2016), SWMM was selected as the top software for modeling the TBW study area. SWMM hydrologic capabilities include but are not limited to estimating runoff, infiltration, evaporation of rainfall, and performance of LID controls. The hydraulic components consist of allowing "unsteady, non-uniform flow routing [through the conveyance system], flow regimes such as backwater, surcharging, reverse flow, and surface ponding" among other methods (Rossman & Huber, 2016). SWMM breaks the urban drainage system into compartments and objects (Table 2-1).

Table 2-1. SWMM's subcatchments and objects that make up an urban drainage system.

Compartments	Description	Representative Object
Atmosphere	• Generates precipitation • Deposits pollutants to Land Surface	• Rain Gauges • Subcatchments
Land Surface	• Receives precipitation from Atmosphere • Outputs evaporation to Atmosphere • Outputs infiltration to Sub-Surface • Outputs surface runoff and pollutant loading to Conveyance	• Subcatchments
Sub-Surface	• Receives infiltration from Land Surface • Groundwater interflow to Conveyance	• Aquifers

Conveyance	• Receives inflows from Land Surface, Sub-Surface, user defined time series
	• Conveys water to outfalls via pipes, channels, pumps, regulators and storage
		• Links
		  ○ Conduits, Flow regulators (weirs, orifices, outlets)
		• Nodes
		  ○ Junctions, flow dividers, manholes, outfalls, storages

Adapted from: Storm Water Management Model Reference Manual Volume 1- Hydrology

2.2.2.1 Personal Computer Storm Water Management Model (PCSWMM)

Approximately ten software packages use SWMM as the engine. The Personal Computer Storm Water Management Model software (PCSWMM), created by the Computational Hydraulics International organization (CHI) was selected for this study. PCSWMM improves the graphical user interface, includes different techniques for

flood modeling, and imports capabilities of various datasets, including GIS layers and Hydrologic Engineering Center River Analysis System (HEC-RAS) stream cross-sections. CHI's mission is to "design urban water systems in a way that supports environmental goals rather than working against them" (CHI, n.d.). PCSWMM allows for large scale modeling with no upper limits on time series data or model objects, very user-friendly, includes tools to assist in modeling such as length and invert estimations, calibration and watershed delineation. Most importantly, PCSWMM supports urban flooding modeling through its comprehensive dual drainage, 1-D, and 2-D modeling of a watershed. The same compartments and objects in Table 2-1 are also used in PCSWMM.

PCSWMM and SWMM are widely used throughout the world for various modeling needs. Moghadas, et al. (2018) used snowmelt modeling in PCSWMM in researching rain on snow events in Sweden to understand urban runoff for current and future climate projections. The model ran event-based simulations for 177 scenarios based on weather conditions, climate change projections, and different infiltration parameters. Research in Australia and Illinois, US used PCSWMM for its hydrologic abilities. The studies looked at the impact of increase of urbanization on runoff quantity and the reduction rate of floods when LIDs are implemented. The Illinois model identified a 32% increase of runoff with a 50-94% increase in urbanization, while LIDs reduced the number of flood events and magnitudes (Ahiablame & Shakya, 2016). The Australian study saw significant hydrologic changes after only a 10% increase of imperviousness, and the implementations of LIDs drastically reduced simulated flood events for 2-year storms from 44 to 2 (Akhter & Hewa, 2016). In a Philippines study,

PCSWMM's 2-D flooding tool was used to model the stormwater network with different scenarios; the results identified that an additional outfall and increased capacity of the main canal would improve the performance of the network and reduce flooding (Liwanag, et al., 2018). All of the studies were able to improve the understanding of flooding in the study areas and could use the model's results to identify and test flood-reducing measures.

Chapter 3. Study Area: Ellicott City, Maryland

3.1 History and Demographics of Ellicott City

Ellicott City, located in Howard County, Maryland, is approximately 30 miles from Washington, D.C., and 10 miles from Baltimore, Maryland. Situated along the Patapsco River, the city began as a milling industry founded by the Ellicott Family. A small community sprouted along the river once the Ellicotts purchased 4 miles of property for their milling business, families, and slaves (Schurman, 2012). Natives soon called the city *The Hollow* due to the steep slopes of the granite rock formation throughout the region (Tyson, 1871). In 1955, the first neighborhood, Normandy Heights, was developed and began further expansion throughout the city upstream of the central downtown district (*The Baltimore Sun*, 1960). Census reports present a 655% increase in population for Ellicott City since 1960 (U.S. Census Bureau, n.d.), The population continued to increase with the most substantial increase happening between 1960-1970 and 1980-1990 (Table 3-1). Aerial imagery of the city reflects the rise in the population through development. Ellicott City's land use has changed from a rural mill town to a developed urban area with historic charm.

Table 3-1. The population of Ellicott City from 1960-2020.

Year	Population	Population Change
1960	9,575	-
1970	17,928	87%
1980	24,274	35%
1990	41,396	71%
2000	56,397	36%
2010	65,834	17%
2020	72,247	10%

Adapted from: U.S. Census Bureau, n.d.

The 30 square miles of Ellicott City, positioned in the Patapsco River Watershed, annually receives 43.4 inches of precipitation on average (HC DPW, 2018). The Patapsco River runs along the northern and eastern side of Howard County, and the upper and lower Patapsco divides the watershed. Ellicott City is located in the Tiber Branch watershed, which is situated in the Lower Patapsco watershed. Compared to the previous century, Maryland is projected to have a 5-10 % change in annual precipitation this century and the former 100-year storm will likely occur every 20-50 years by 2100 (Runkle, et al., 2017). There are seven major recorded floods in Ellicott City from 1868 with four related to hurricanes and tropical storms and the two most recent flash floods in 2016 and 2018 caused by brief extreme precipitation (USACE Baltimore District, 2020).

3.2 Tiber Branch Watershed

The Tiber Branch Watershed is a 3.8 square mile watershed that comprises 3 main tributaries, Hudson, Tiber, and New Cut (Figure 3-1). The Hudson Branch begins in the northern region of the watershed spanning US-40 and US-29, then flowing along Frederick Road and Main Street in natural and concrete channels before converging with the Tiber Branch in a parking lot in Old Ellicott City. The Tiber Branch commences on the western side of U.S. 29, upstream of I-70. The stream crosses US-29 and flows through residential regions before merging with the Hudson Branch. New Cut Branch begins in the southern province of the watershed and flows northeast along New Cut Road and joins with the Tiber-Hudson Branch behind building-lined Main street before flowing into the Patapsco River.

Starting as an industrial production town, the progress of the Baltimore and Ohio Railroad in the 1820s transformed the terrain with the construction of railways throughout the mountains and forests, therefore reforming the hydrologic terms of the watershed (HC DPW, 2018; Stover, 1987). With the increase of the population, the Tiber Branch observed an abundance of transformations in its headwaters. With the booming economy and society, 40% of the land is now residential; the land use breakdown is summarized in Table 3-2. Aerial imagery from 1963-2017 shows the increase in imperviousness through development of business centers and residential development (Figure 3.2). The urbanization of the TBW further changed the landscape of the watershed; most of the stormwater management obligations were constructed before the development occurring, resulting in a stormwater network unsuitable for the growth (HC DPW, 2019).

Table 3-2. Land Use in Tiber Branch Watershed.

Land Use	Percentage of Land (%)
Residential	40
Non-Residential	32
Open Space	18
Undeveloped	10

Reproduced from: Howard County Department of Public Works, 2019

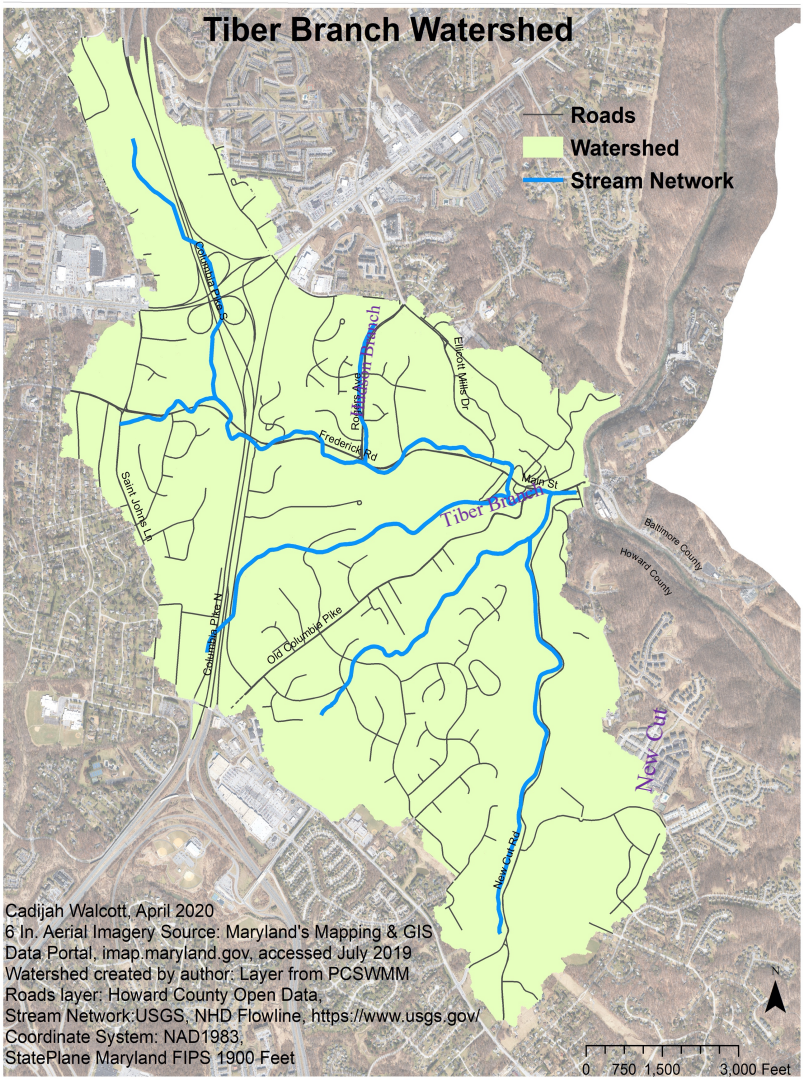

Figure 3-1. The Tiber Branch Watershed discharging to the Patapsco River at Main Street, Ellicott City.

The three main rock formations in the TBW are: Baltimore Gabbro Complex, Ellicott City Granodiorite, and Oella Formation; coupled with the intersection of the Piedmont and Coastal Plains (the Fall Line), they form the steep slopes of the city (HC DPW, 2019). The 43 soil types in the TBW are displayed in Figure 3.2 (specific details in Appendix A).

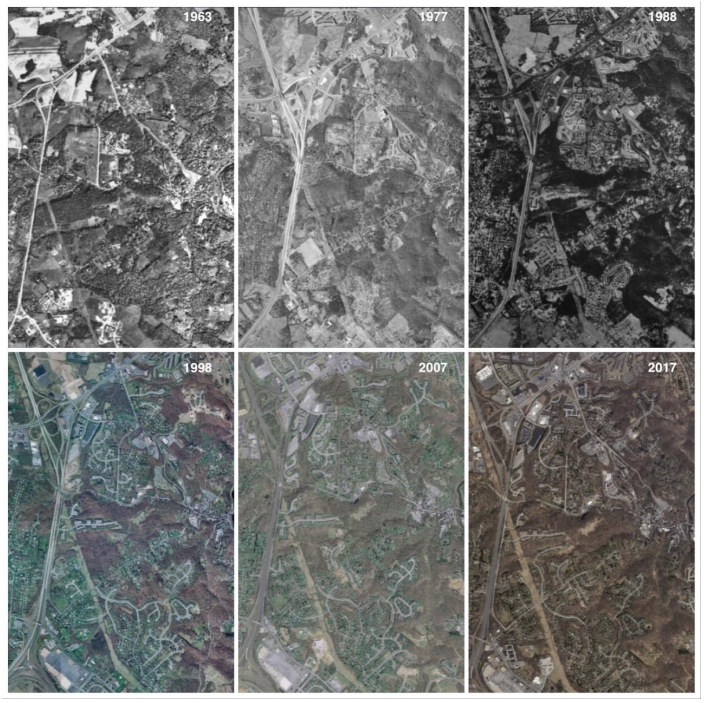

Figure 3-2. Aerial Imagery of Tiber Branch Watershed from 1963-2017.

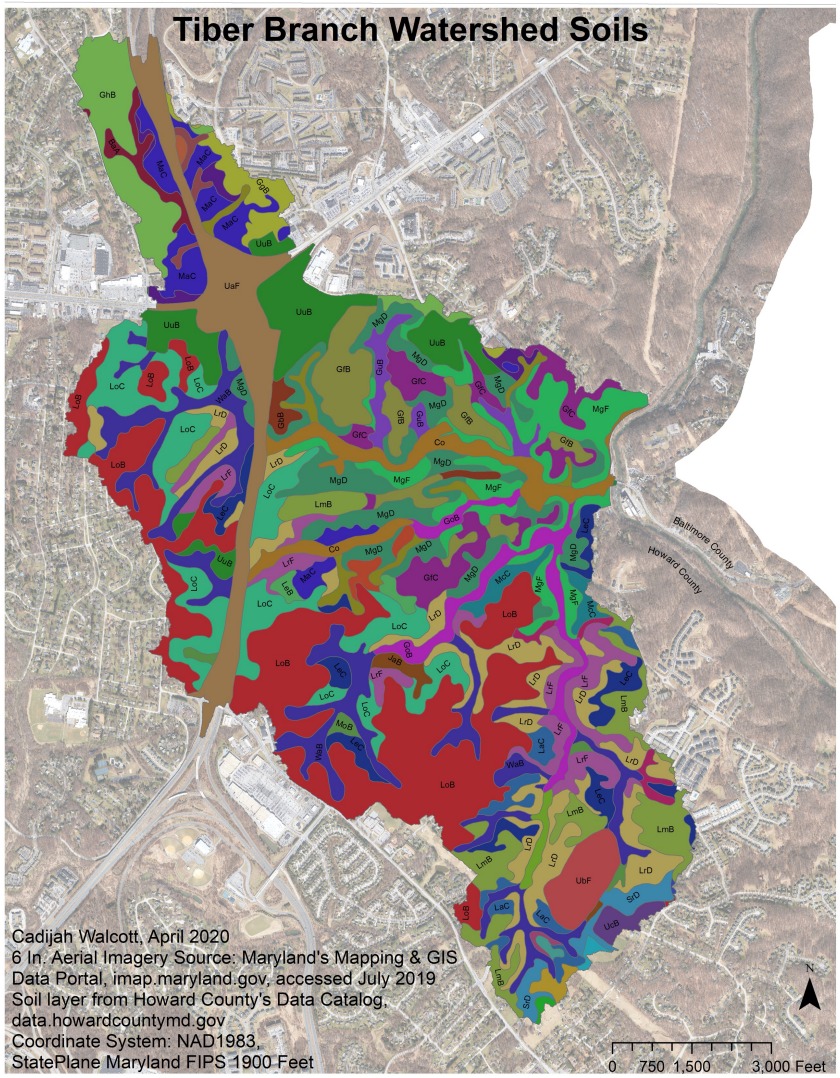

Figure 3-3. The distribution of the 43 different soil types in the Tiber Branch Watershed.

Chapter 4. Model Development

This chapter discusses the necessary steps to set up the TBW model in PCSWMM. As mentioned in Chapter 3, SWMM separates the model into four compartments: Atmosphere, Land Surface, Sub-Surface, and Conveyance. These four compartments form the features of an urban drainage system, but all are not required. The TBW model developed in this thesis employed three compartments: the Atmosphere, Land Surface, and Conveyance. The Sub-Surface compartment receives infiltration from the Land Surface compartment and translates to groundwater and stored in an aquifer. This compartment was not included in this model, and it is expected that some runoff errors occurred because of this decision.

4.1 Simulation Options

SWMM provides various options to fit the needs of different models; this includes being able to choose the process model, routing method, and infiltration model in the simulation options. Additionally, the simulation options allow changes to dates to match time series and reporting and routing time steps.

4.1.1 Process Models and Routing Methods

The rainfall-runoff and flow routing process models are used for modeling urban flooding, where surface runoff is the issue being researched. Other possible options include snowmelt, groundwater, and water quality, but they do not pertain to this model and were not included in this explanation. SWMM's dynamic rainfall-runoff simulation creates the hydrologic input for the model from the inputted hyetograph and

characteristics of the subcatchments. Subcatchments are treated as storages with inflows and outflows. The outflows are considered infiltration, depression storage, and evaporation, while inflow is the incoming precipitation. Surplus from the difference of inflows and outflows is rainfall excess; when the subcatchment reaches capacity, runoff is produced. SWMM transformation of subcatchment discretization into rectangular shapes with uniform flow, width, and slope simplifies calculations for runoff by using Manning's equation to calculate runoff as a flow rate in Equation 4.1.

$$Q = \frac{1.49}{n} * W * \sqrt{\bar{S}} * (d - ds)^{\frac{5}{3}} \qquad 4\text{-}1$$

Where Q is the runoff flow rate (cfs), W is the width of subcatchment or average length of the flow path (ft), n is Manning's roughness coefficient, S is the average slope (ft/ft), d is the ponding water depth (ft), and ds is depression storage (ft).

Flow routing is the second process model employed to replicate the hydraulic element of the model. SWMM uses the conservation of mass and momentum to model the movement of water through natural channels (swales, streams, rivers) and the stormwater network. Assuming the flow is unsteady and non-uniform, the Saint Venant equations used are:

$$\frac{\partial \mathrm{A}}{\partial \mathrm{t}} + \frac{\partial \mathrm{Q}}{\partial \mathrm{x}} = 0 \qquad \text{Continuity} \qquad 4\text{-}2$$

$$\frac{\partial \mathrm{Q}}{\partial \mathrm{t}} + \frac{\partial}{\partial \mathrm{x}}\left(\frac{Q^2}{A}\right) + gA\left(\frac{\partial \mathrm{H}}{\partial \mathrm{x}}\right) + gAS_f = 0 \qquad \text{Momentum} \qquad 4\text{-}3$$

where Q is the discharge (cfs), A is the cross-sectional area of the conduit (ft^2), x is the distance (ft), t is the time (sec), H is the hydraulic head of the flow (ft), g is the acceleration of gravity (32.2 fps), and S_f is the friction slope (ft/ft).

Different versions of the Saint Venant equations are used to solve different routing methods: steady flow, kinematic wave, and dynamic wave. Dynamic wave is the optimal option for the routing method for urban flooding, given that it can replicate flow reversal, pressurized flow, and backwater effects, which are significant causes of urban flooding. While steady flow and kinematic wave routing methods partially use the Saint Venant equations, dynamic wave routing utilizes the entire equations for the most accurate and advanced option for urban flooding (Rossman & Huber, 2016). The TBW consists of stormwater drainage network and overland flow co-occurring; therefore, the dynamic wave analysis was the only flow routing option suited for modeling the complexities of the system. When using the dynamic flow routing option, 0.5 second routing time steps were used for numerical stability; this setting, unfortunately, also increased the computational time.

4.1.2 Infiltration Method

PCSWMM supports three infiltration methods: Horton, Green Ampt, and Curve Number (CN). The CN method is widely used in practice in Maryland and was selected as the infiltration method for the TBW. The United States Department of Agriculture's (USDA) Soil Conservation Survey (SCS), now known as the Natural Resources Conservation Service (NRCS), created the CN method to estimate the quantity of runoff that is produced from rainfall with a loss concept; it is expressed in equations 4-4 thru 4-6.

$$Q = \frac{(P - I_a)^2}{(P + 0.8S)} \qquad 4\text{-}4$$

$$I_a = 0.2 * S$$

4-5

$$S = \frac{1000}{CN} - 10 \quad \text{4-6}$$

where Q is runoff (in.), P is precipitation (in.), I_a is initial abstractions (in.), S is maximum potential retention (in.), and CN is curve number. For the TBW model, CN was calculated by subcatchment as described in section 4.3.1.2.

4.1.2.1 Hydrologic Soil Groups

The Hydrologic Soil Group (HSG), which determines the potential of water interception through a soil's layers, is grouped into 4 categories, from greatest to least capacity to absorb water (least to greatest tendency to generate runoff): A, B, C, and D. Grouping is based on characteristics of the soil and the saturated hydraulic conductivity (Ks) which quantitatively measures a "saturated soil's ability to transmit water through its pores under certain conditions" and represents the slope of the relationship between the soil's hydraulic gradient and water flux (USDA, n.d.). Descriptions of HSG are in Table 4-2, and standard saturated hydraulic conductivity values are in Table 4-3. Based on a 2003 soil survey completed by National Cooperative Soil Survey for Howard County, the TBW encompasses 43 different soil types and all four HSGs (USDA 2003). The NRCS's Soil Survey Geographic database's (SSURGO) Mapunit Aggregate Attribute Table (muaggatt) (NRCS, 2020) was used to distinguish the different HSGs for the soil types. Some soils are assigned dual HSGs, determined by the distance to the water table. If the distance is within 24 inches, a D added is the soil type, such as A/D, B/D, or C/D. For the purpose of this research, only one HSG was assigned to each

soil, as determined by muaggatt and soil survey details. Figure 4-2 displays the distribution of HSG throughout the TBW.

Table 4-1. Hydrologic Soil Group's classifications based on runoff potential, composition, and soil texture.

HSG	Runoff Potential	Composition	Soil Texture
A	Low	Less than 10% clay, greater than 90% sand or gravel	Loamy sand, sandy loam, loam or silt loam
B	Moderately Low	10 & 20% clay, 50-90% sand	Loamy sand, sandy loam
C	Moderately High	20 & 40% clay, less than 50% sand	Sandy clay loam, loam, silt loam, clay loam, silty clay loam
D	High/Highest	Greater than 40% clay, less than 50% sand	Clayey

Note: Adapted from (United States Department of Agriculture, 2007)

Table 4-2. Saturated hydraulic conductivity (Ks) for the least transmissive layer for two types.

Type	HSG A	HSG B	HSG C	HSG D
A	> 5.67 in./hr	1.42 – 5.67 in./hr	0.14 – 1.42 in./hr	< 0.14 in./hr
B	> 1.42 in./hr	0.57 – 1.42 in./hr	0.06 – 0.57 in./hr	< 0.06 in./hr

Type A: Depth to water-impermeable layer is 20-40 inches, and depth to the high-water table is 24-40 inches. Type B: Depth to water-impermeable layer and high-water table is greater than 40 inches
Note: Adapted from (USDA, 2007)

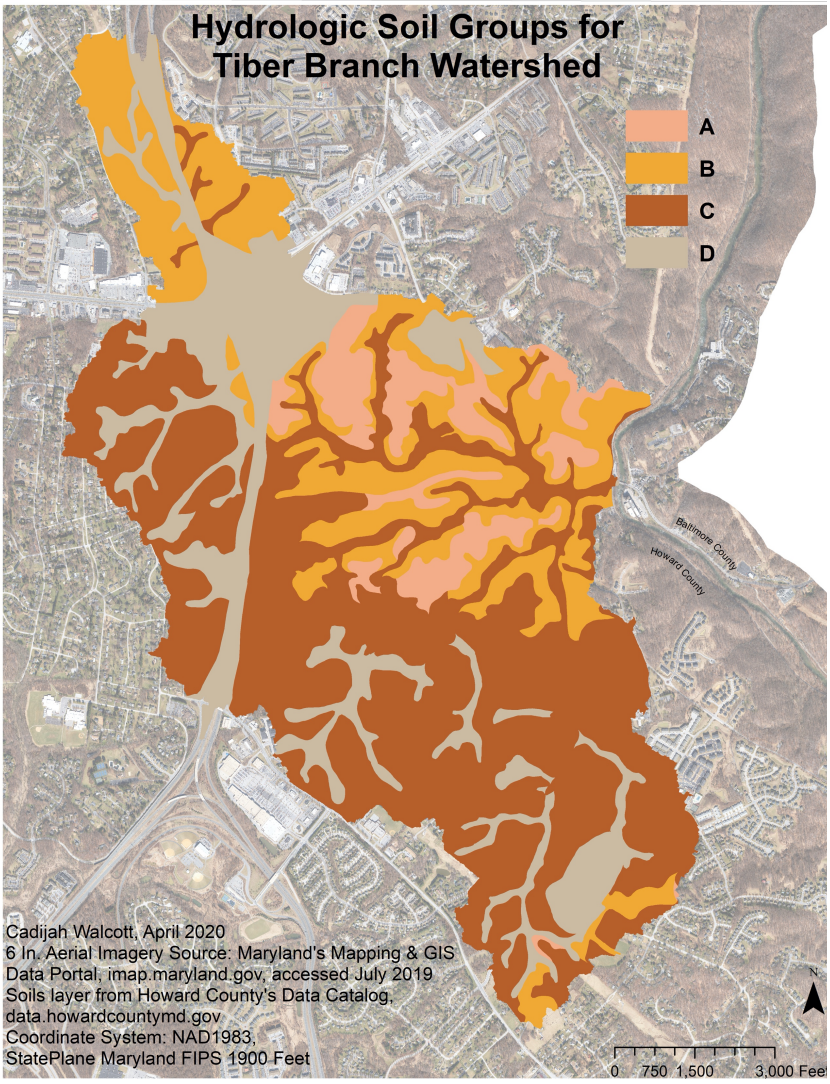

Figure 4-1. Hydrologic Soil Groups in Tiber Branch watershed.

4.1.2.2 Drying Time

Soil moisture in a continuous model is adjusted to account for the time it takes saturated soil to dry. SWMM's hydrology manual suggests that drying time is related to Ks and is governed by Equation 4.9:

$$T = \frac{3.125}{\sqrt{\overline{Ks}}} \qquad 4\text{-}8$$

where T is drying time (days) and Ks is saturated hydraulic conductivity (in/hr).

The drying time for the CN infiltration method recovers the S in Equation 4-6. The maximum potential retention is replenished after an event has depleted it. The United States Geological Survey (USGS) provides tabular data for area and depth weighted averages for SSURGO variable in the United States (Wieczorek, 2014). The vertical hydraulic conductivity was used, and the units were converted to inches per hour. This dataset was merged with the soils layers and the drying time was calculated for each SSURGO soil in the TBW and an area weighted average was calculated for each subcatchment.

4.2 Atmosphere Compartment

The Atmosphere compartment "generates precipitation and deposits pollutants onto the Land Surface compartment" (Rossman & Huber, 2016). The model developed in this study is for flooding (water quantity) concerns and not water quality; thus, pollutant concentrations were not involved.

4.2.1 Precipitation

SWMM can generate hyetographs or accept different formats for input in the model. For this model, the precipitation data were downloaded from Howard County's database for rain gage, Ellicott City 8197, located near Brightwell Drive and Court House Drive. Ellicott City 8197 is the only rain gage in the watershed. The precipitation was assumed uniform throughout the watershed for this model; this assumption may not reflect actual conditions. Rainfall depth from January 1, 2018, to December 31st, 2019, was used for the rain gage in PCSWMM; this time series is shown in Figure 4-2.

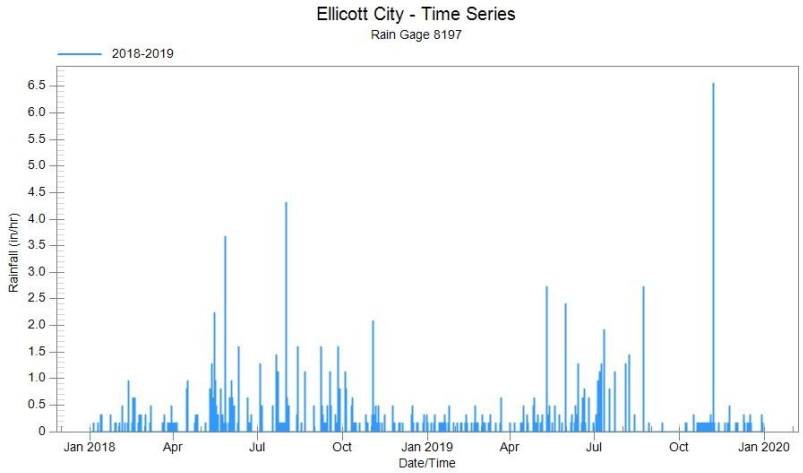

Figure 4-2. Rain hyetograph for 01/01/2018 to 12/31/2019 for Ellicott City 8197 rain gage.

4.2.2 Evaporation

Evaporation is a part of the outflow process for calculating runoff from a subcatchment in SWMM and is necessary input for the model to reduce runoff continuity error. The rate of depletion of water from impervious depression storages is calculated based on evaporation. Monthly evaporation data for Maryland was downloaded from NOAA's National Centers for Environmental Information (NOAA, 2018) for April – October 2018 (Table 4-3). During the months of November – March, evaporation rates are reduced due to lower temperatures and moisture; data for those months are not included.

Table 4-3. 2018 monthly evaporation data for the State of Maryland.

Month	Evaporation (in.)
April	4.37
May	5.42
June	5.56
July	7.49
August	5.99
September	3.76
October	3.30

Source: Downloaded from (National Oceanic and Atmospheric Administration, 2018)

4.3 Land Surface Compartment

The Land Surface compartment receives precipitation and evaporation data from the Atmosphere compartment and partakes in the inflows and outflows calculations of runoff for each subcatchment.

4.3.1 Subcatchments

SWMM performs hydrologic calculations for segments of the watershed called subcatchments, also referred to as sub-basins and sub-watersheds. SWMM's subcatchments are irregularly-shaped polygons with varying properties, mathematically defined by the model's parameters. SWMM applies precipitation data to each subwatershed to compute that area's hydrologic input through the rainfall-runoff process. SWMM streamlines the calculations by using a "nonlinear reservoir model to estimate surface runoff produced by rainfall" (Rossman & Huber, 2016). Each subcatchment acts as a reservoir receiving inflow (precipitation) and producing outflow (runoff, evaporation and infiltration). Each is subdivided into three sub-areas: impervious, pervious, and impervious with no depression storage.

With advances in technology and the availability of datasets, an analyst is no longer required to rely solely on topographic maps to delineate watersheds in urban areas. PCSWMM creates subcatchments with its Watershed Delineation tool using a digital elevation model (DEM) of the region, burning[1] the stream network and stormwater drainage network into the DEM, and accepting user-defined locations of subwatershed outlets. Subcatchment outlets were identified by stormwater inlets and the stream network. With fine-tuning, the Tiber Branch Watershed was subdivided into 1,359 subcatchments with an average size of 1.79 acres and average slope of 15.6% (Figure 4-3). The green subcatchment on the eastern side of the watershed is large (87 ac) due to lack of data on the stormwater drainage network in that region thus assuming

[1] Burning the stream and stormwater network into the DEM layer is the process of decreasing the elevation of the stream and stormwater network to force flow accumulation to those locations. This process was completed in PCSWMM but can also be completed using GIS tools.

all the runoff in that region flows to the same outlet. GIS tools embedded in PCSWMM calculated the area (ac), width (ft), and average slope for each subcatchment. Percent of Impervious Area, Manning's roughness for overland flow for pervious and impervious areas, depression storage for pervious and impervious areas, and infiltration parameters were all calculated or estimated using other tools as described below. As an alternate approach, the subcatchments were also delineated in ArcMap; that process is detailed in Appendix B. Ultimately, the PCSWMM-derived subwatersheds, not the ArcMap-analyzed ones, were used in the TBW model.

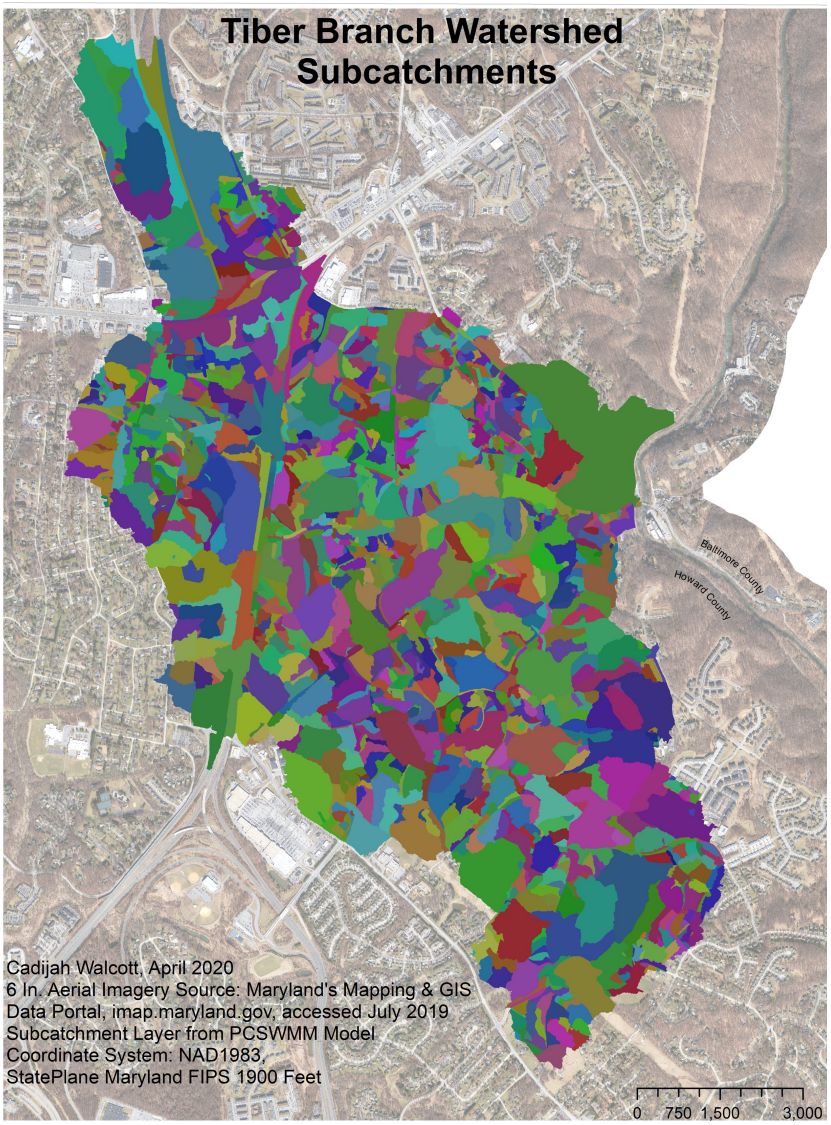

Figure 4-3. Subcatchments for the Tiber Branch Watershed.

4.3.1.1 Percent of Impervious Area

Percent of impervious area is a required input value for each subcatchment. Roads, buildings, and driveway polygons were downloaded from Howard County's Open Data website (Howard County, 2020) to calculate the percent of impervious area in each subcatchment and the watershed. Employing GIS tools (merge, editor's merge tool, intersect, dissolve), these three polygon layers were combined with no overlap to create a single impervious layer that was used for calculating the percent of impervious area for each subcatchment (Figure 4-4). Based on this layer, 26.6% of the TBW area is impervious.

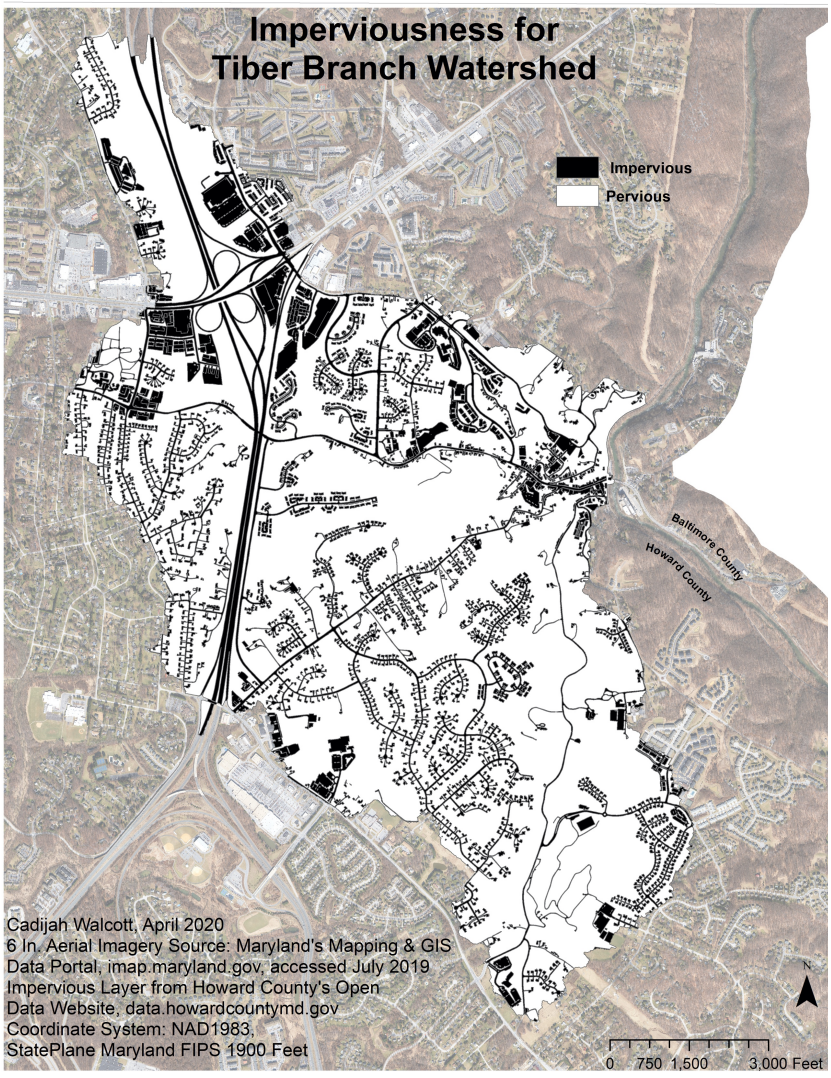

Figure 4-4. Imperviousness in Tiber Branch Watershed.

4.3.1.2 Curve Number Calculations

A CN is a dimensionless variable that typically ranges from 30 to 100 and represents the potential of runoff based on the HSG, land use, hydrologic conditions, and imperviousness. The CN determines the maximum potential retention, S, in equations 4-2 through 4-4, for each subcatchment. The impervious layer (Figure 4-4), HSG (Figure 3-1), and subcatchment (Figure 4-3) layers were intersected (GIS Tools: intersect, dissolve, editor's merge) and used to calculate the CN. If a resulting polygon was classified as impervious, it received a curve number of 98. If it was a pervious polygon, the CN was assigned based on HSG (Table 4-4). All pervious areas were considered open space in good conditions under Antecedent Conditions II. An area-weighted CN was calculated for each subcatchment using Equation 4-7:

$$CN_w = \sum \left(\frac{A_i}{A_s} * CN_i \right) \qquad 4\text{-}7$$

where CN_w is the weighted CN corresponding to a specific subcatchment, A_i is the area of the polygon corresponding to a specific curve number (ac), A_s is the area of subcatchment (ac), and the sum is taken over the number of polygons contained in the subcatchment.

Table 4-4. Curve numbers for impervious and pervious areas.

HSG	Impervious CN	Pervious CN
A	98	39
B	98	61
C	98	74
D	98	80

Note: Adapted from (United States Department of Agriculture, 1986)

A land use layer was available for download but ultimately was not used because it did not reflect current land use, and instead, reflected ultimate land-use based on zoning. Additionally, CN formulations based on land use are derived using assumptions about impervious area fraction (USDA, 1986), and in this case, a detailed impervious map was available. Thus, the impervious layer was used as described in this section; the resulting curve number distribution for TBW is shown in Figure 4-5.

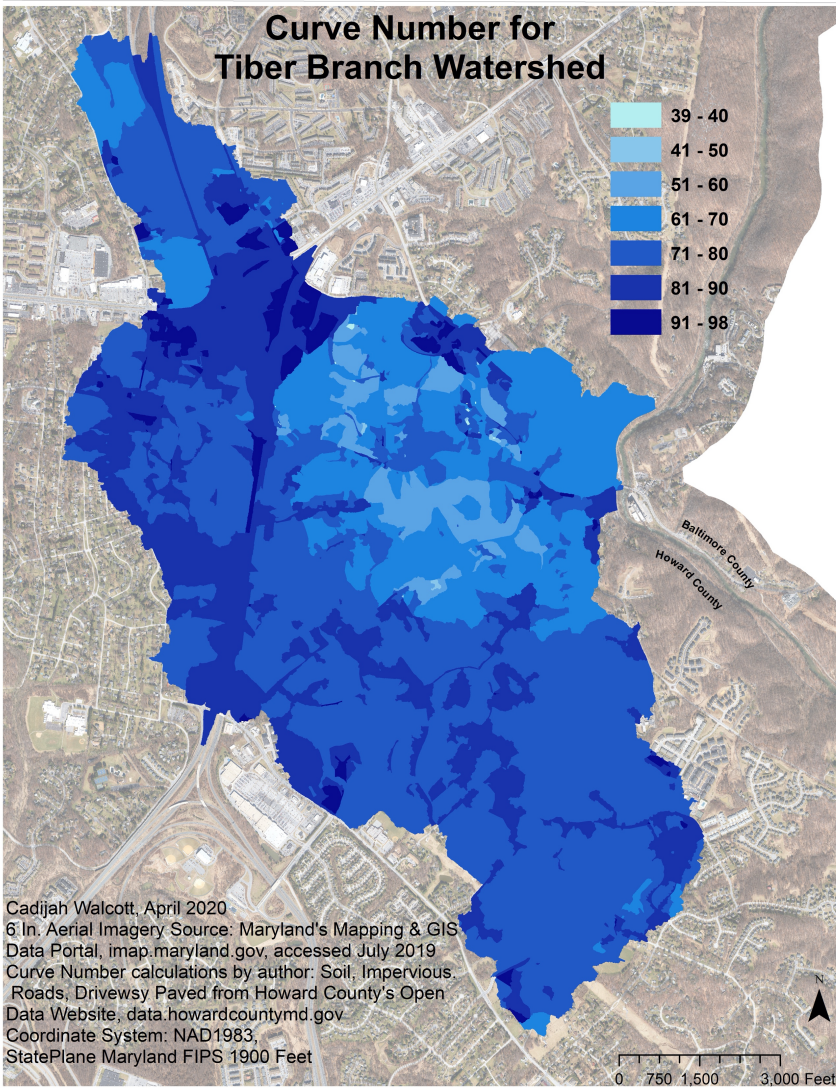

Figure 4-5. Curve Number by Subwatershed for Tiber Branch Watershed (Subwatershed boundaries are not shown).

4.3.1.3 Manning's Roughness Coefficient

Manning's roughness coefficient (MRC), n, is a parameter classifying the roughness of a surface and its interaction with the flow of precipitation, which can impact time of concentration and time of peak. In practice, it is challenging to estimate roughness as a result of "considerable variability in landscape features, transition between laminar and turbulent flow, very small flow depths" (Rossman & Huber, 2016). As surface roughness increases, the time of concentration and infiltration increase, and the peak of the hydrograph decreases. The NRCS recommended values are used for the pervious and impervious areas. There is considerable uncertainty in estimating MRC values for overland flow. Roughness values initially used are in Table 4.5 and may change in the calibration process. MRC was set to zero for pervious areas when using the curve number infiltration in SWMM to estimate runoff "to prevent delay of runoff flow" (Rossman & Huber, 2016).

Table 4-5. Manning's Roughness Coefficient for Overland Flow.

Type	Manning's Roughness Coefficient
Pervious Overland Flow	0.24
Impervious Overland Flow	0.011

Source: (Rossman & Huber, 2016)

4.3.1.4 Depression Storage

Depression storage is an average depth that represents the small-scale storages within impervious and pervious areas; it is included in the nonlinear outflow calculations for the idealized subcatchments. Precipitation stored in the pervious depression storage depletes by infiltration and evaporation and precipitation stored in impervious areas depletes only by evaporation, inducing a longer time to depletion

(Rossman & Huber, 2016). The treatment of depression storage in SWMM varies with the user's choice of infiltration method. Pervious depression storage was set equal to the initial abstractions calculated in Equation 4-5 (Rossman & Huber, 2016). Accurately quantifying depression storage values is challenging; a multitude of estimates for this parameter are available. Recommended values were entered for each subwatershed; it was anticipated that this parameter would be a candidate for adjustment in calibration.

4.4 Conveyance Compartment

The Conveyance compartment receives input from the land surface compartment in the form of runoff and routes flow through the stormwater and stream network. The Conveyance compartment represents the hydraulic portion of the model; it includes two SWMM object types: links and nodes. Links in a SWMM model include conduits in a stormwater drainage network, roadways, streams, weirs, orifices, and outlets. Nodes in the model are the connection for links and are represented by junctions, storages, and an outfall. A junction is further distinguished as a stormwater inlet, manhole, dual drainage node or location of stream's cross-section change, explained in further detail below. Howard County's stormwater geodatabase was utilized to identify the location of links and nodes. Table 4-6 shows the allocation of links and nodes.

Table 4-6. Inventory of SWMM objects in the Conveyance Compartment.

SWMM Object	Count
Node - Inlet	865
Node - Manhole	404
Node - Stream	682
Node - Dual Drainage	1,069
Node - Storage	61
Node - Outfall	1
Link - Stream	307
Link - Stormwater Pipes	1,366
Link - Roadway transect	761
Link - Weirs	79
Link - Orifices	48
Link - Outlets	1,017

Howard County's stormwater geodatabase includes the subsurface pipes, stormwater inlets and manholes, drainage channels, and various LIDs. PCSWMM imports GIS layers and creates objects from the features but only provides the location and does not include parameter estimations for SWMM objects, such as invert elevation and inlet and outlet's node or offset. The geodatabase includes unique naming for individual features but does not include connectivity or direction of flow information. There are more than 7,300 objects in the conveyance compartment of this model. Each object's parameters were estimated by reviewing as-builts provided by Howard County and Maryland's State Highway Administration; the information was inputted manually.

4.4.1 Link: Conduits in The Stormwater Drainage Network

The TBW model includes 1,366 links that symbolize pipes in the underground stormwater drainage network. A conduit's essential input properties include upstream and downstream nodes, cross-sections shape and dimensions, inlet and outlet offset

from the invert elevations of connected nodes, MRC, and length. SWMM uses the provided inputs to estimate flow rate and depth using Manning's equation. The program calculates slope in the Manning's equation using the inlet and outlet offset from connected nodes.

As-built drawings were provided by Howard County's Stormwater Division to supply necessary information needed for the conduits; if the data were not available, conduit parameters were estimated based on surrounding conduits. If that was not possible, site visits were completed. Howard County's interactive map displayed the drainage network and provided some data, but, in some cases, it was incomplete. For example, the culvert connection between the stormwater drainage network flowing down Rogers Ave and toward the Hudson Branch tributary (Figure 4-6) was missing in the interactive map. A site visit was necessary to accurately estimate the properties of the missing conduit. The pink dots and lines in Figure 4-6 represent the stormwater network. Figure 4-7 indicates that the missing conduit is actually two conduits at different offsets from the upstream node and the location where it enters the stream.

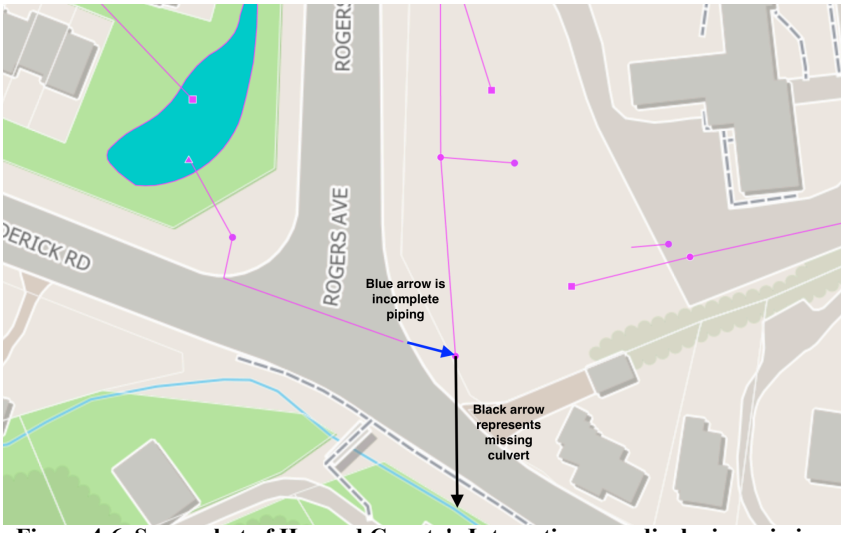

Figure 4-6. Screenshot of Howard County's Interactive map displaying missing data.

Figure 4-7. Image from site visit investigating the missing conduit in the Howard County's Interactive Map.

4.4.2 Link: Stream Channel

Detailed data for the stream network was vital to accurately characterize flow and depth in the stream. Maryland's Digital Flood Insurance Rate Maps (DFIRM) Outreach Program, MDFloodMaps (MDE, 2020) provided HEC-RAS models of the Tiber Hudson Branch, New Cut Branch, Autumn Hill Branch, and Cat Rock Run tributaries. The HEC-RAS data were imported into PCSWMM and converted to links and nodes to represent the stream channel throughout the model (Figure 4-8).

Each imported HEC-RAS cross-section of the stream was translated in PCSWMM into a transect that represents the stream channel conduit (link). For example, Figure 4-9 illustrates the transect for Conduit CJ6039 on the Tiber Hudson Branch tributary.

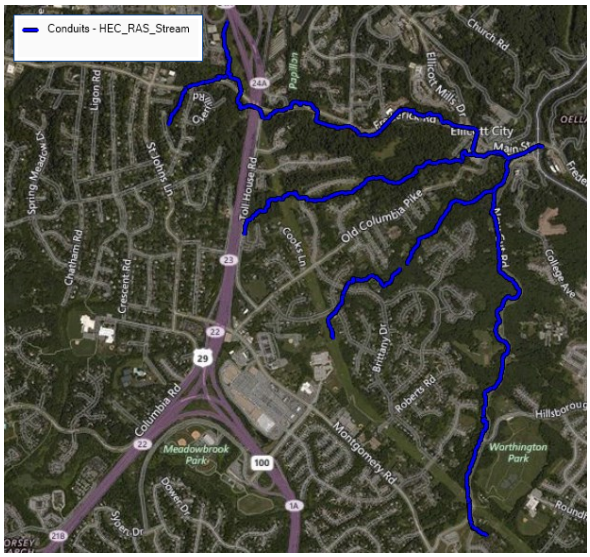

Figure 4-8. HEC-RAS Model of Tiber Branch watershed streams imported into the PCSWMM model.

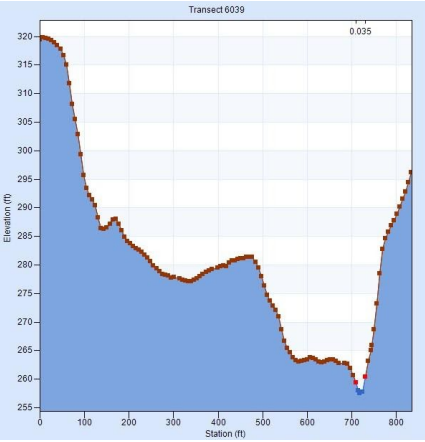

Figure 4-9. Transect of Conduit CJ6039 showing the stream channel.

To connect flow from the storm drain network to the stream channels, tributaries without existing hydraulic models were estimated. The USGS National Hydrography Dataset (NHD) provides spatial line features that denote the paths of streams and rivers. In some cases, the NHD flowline was not precisely placed in the watershed based on the local DEM layer and high-resolution aerial imagery provided from Maryland's Mapping & GIS Data Portal (MD iMap, 2020). In such cases, the NHD flowline was edited to match the DEM and imagery using GIS tools. Figure 4-10 shows an unedited portion of the NHD Flowline and the edited NHD Flowline with the DEM layer in the background. The white lines represent contours to easily see the location of the stream. The black dots represent the junctions along the stream network in PCSWMM and were used to guide the flowline. The light blue line represents the NHD flowline before edits and the darker blue lines are after edits but before it is saved. While the unedited flowline gave the general location of the river, it was not exact, and

Commented [KLB1]: This figure is fuzzy and doesn't illustrate the process convincingly. Can you make it higher res or find a better one?

this editing process ensured that tributaries were flowing in topographically consistent paths in the model.

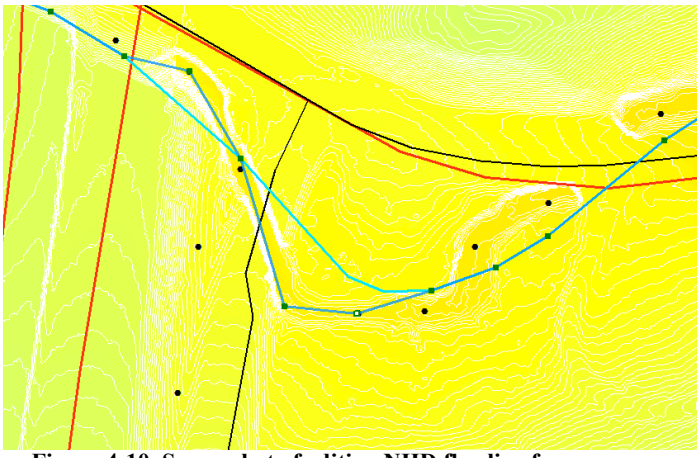

Figure 4-10. Screenshot of editing NHD flowline for accuracy.

The NHD flowline and DEM provided centerline locations for missing tributaries; the model also requires a channel cross-section. A standard cross-section was used to estimate the missing data (illustrated in Figure 4-11). The cross-section is for a natural channel with a trapezoidal shape, where side slope z is equal to 3, d represents the maximum depth of water, and b is the bottom width of the stream. Depending on the location of the added stream, b was set to 3 or 6 feet, and the maximum depth was set to 5 feet. The bottom width was chosen based on how many smaller tributaries were combined to flow as one. Further field visits would allow more accurate specification of small-tributary cross sections.

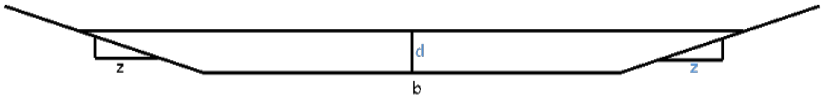

Figure 4-11. Smaller tributary cross-section for stream reaches where no HEC-RAS model is available.

4.4.3 Link: Flow Regulators —Weirs, Orifices, and Outlets

Flow regulator links (weirs, orifices, and outlets) adjust the flow under certain conditions. The TBW model includes 79 weirs, 48 orifices, and 1,017 outlet links; 15 of the weirs simulate emergency spillways. All but one weir act to regulate flow from a stormwater detention pond to the stream network. Weirs representing emergency spillways and high flow through a pond's riser are represented as trapezoidal and transverse weirs, respectively. Orifices regulate the low flow and determine the pond's initial water depth. SWMM applies standard rating curves to model hydraulic performance of weirs and orifices (Rossman & Huber, 2016). Required inputs for orifices and weirs include offset height from the pond's bottom, which determines the low flow and high flow, cross-section shape and dimensions of the opening, and discharge coefficient. Detailed design and as-built drawings were available for some stormwater ponds in the watershed; link parameters were taken from those drawings. If the data were not available, details were estimated based on ponds with similar sizes and their link characteristics. Standard discharge coefficients in SWMM's manual

displayed in Table 4-7 were used in the model based on characteristics of the flow regulator link.

Outlet links are used in Dual Drainage modeling (explained in Section 4.5) to regulate the flow in a stormwater inlet to the surface, mimicking pressurized backflow. Various stormwater inlets are installed in the TBW; for simplicity, the dimensions of the most common inlet, a Howard County Type A-10, were used to establish all outlets' rating curves in the model. Howard County's Design Manual (HC DPW, 2020), Federal Highway Administration's Urban Drainage Design Manual (FHA, 2013) and site visits provided the information needed to estimate the rating curve for the Type A-10 inlet. The resulting rating curve for a discharge-depth relationship is given by Equation 4.8, where Q is discharge (cfs), and y is depth (ft).

$$Q = 4.634 * y^{1.491} \qquad 4\text{-}8$$

Table 4-7. Discharge coefficients for weirs and orifices used in the SWMM model.

Flow Regulator Link	Discharge Coefficient
Weir - Trapezoidal	2.9
Weir - Transverse	3.33
Orifice	0.65

Source: (Rossman & Huber, 2016)

4.4.4 Junction Node: Manholes, Stormwater Inlets, Dual Drainage, Stream & Outfalls

Junction nodes are used to connect links, such as streams and conduits, for flow continuity. Junction nodes along the stream network connect two streams with differing cross-sections; they were created when importing the HEC-RAS cross-sections. Junction nodes in the stormwater network, inlets and manholes, are treated identically in terms of their properties, but they have conceptually different roles. Stormwater inlets are considered outlets for overland flow from subcatchments; they receive the runoff hydrograph from the subcatchments, and thus connect the Land Surface compartment to the Conveyance compartment. Manholes are solely for the transport of flow between pipes (links) in the storm drain network. The input parameters for inlets and manholes include invert elevation, depth, ponded area, and surcharge depth. Ponded area is an optional parameter that accounts for water accumulation on the surface when the node is flooded; without the specification of this parameter, the water would be lost from the system.

SWMM's dual drainage configuration allows the model to simulate surface flow in gutters and roadways when the underground conduits (storm drains) are surcharged; the dual network is a replica of stormwater inlets and downstream manholes along roadways and labeled with the same name, but with an "-S" added at the end. The dual drainage nodes and its subsurface partners are connected by an outlet link that regulates the flow between the two nodes.

The outfall node is the final location for flow in the model. It is located at the Main Street entrance to the Patapsco River, just downstream of the Frederick Road overhead bridge. The outfall's input parameters include invert elevation and type.

4.4.5 Storage Node: Stormwater Detention Ponds

Storage nodes in SWMM are the only nodes with capacity to accumulate and release water volume; they are characterized by stage-storage data that represent the volume stored at different depths. In this model, 61 storage nodes symbolize 54 storm-water detention ponds and 7 underground storage tanks. The storage nodes receive inflows from the stormwater network and discharge outflows via weirs and orifices. The primary input parameters incorporate invert elevations, maximum depth, and tabular data detailing depth and surface area for the pond and tanks. Ponds and tanks were identified using Howard County's Interactive Map, as-built plans, and the local DEM layer. GIS tools were used to obtain pond specific elevation data to confirm invert and maximum depth from as-builts and to estimate them when data was not available. ArcMap's 3D Analyst tool was used to calculate the surface area of the pond for an incremental set of depths. The surface area – depth relationship is stored in a storage curve table which SWMM uses to calculate a pond's volume (storage) using trape-zoidal rule integration. Figure 4-12 displays the identified stormwater detention ponds used as storage nodes. Detailed steps are provided in Appendix C (GIS Tools Used: Create Feature Class, Extract by Mask, Area and Volume toolbar

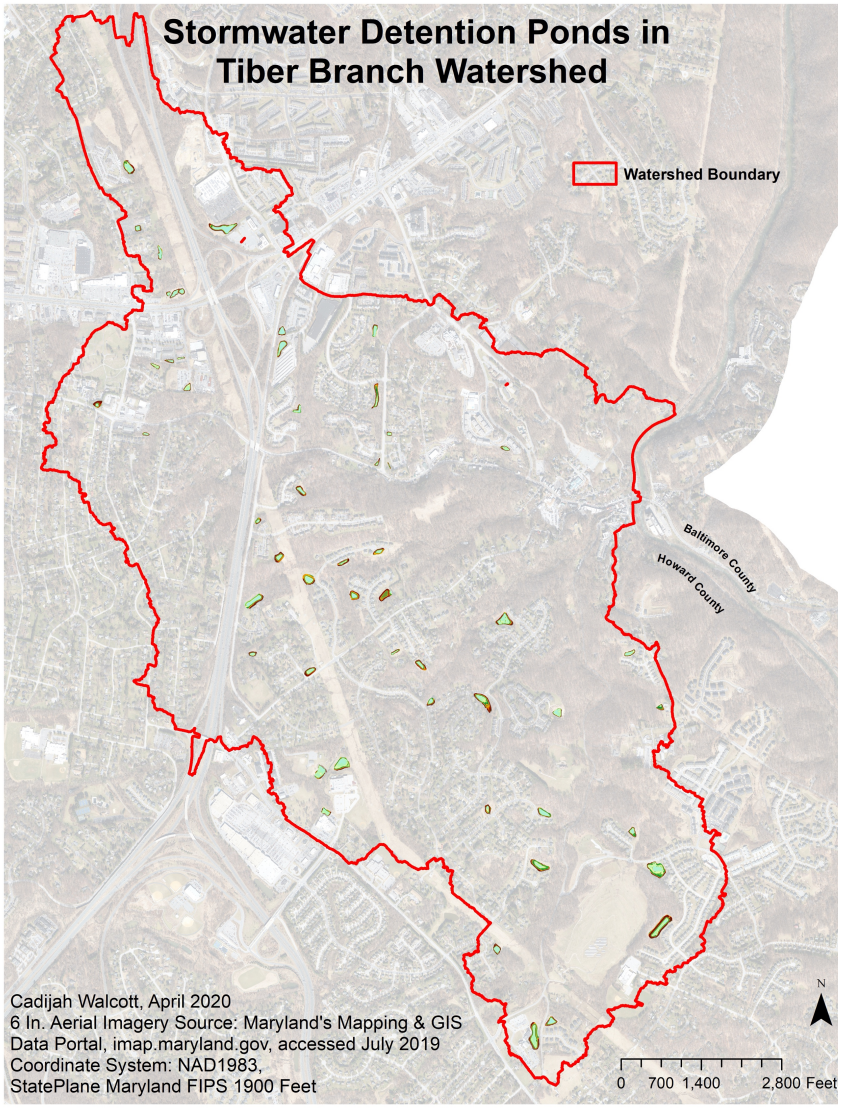

Figure 4-12.Stormwater detention ponds in Tiber Branch Watershed.

4.5 Dual Drainage

Urban flooding occurs when stormwater networks are overwhelmed, and excess precipitation accumulates in roadways, ditches, and floodplains. The relationship between the stormwater drainage network and overland flow is essential to understanding urban flooding in the TBW. It was modeled using SWMM's dual drainage system, which includes minor and major systems. The minor system is the underground stormwater drainage network, including conduits, inlets, and manholes. The major system is overland flow in roadways, ditches, and floodplains. At every location where such conditions might occur, the two systems are connected by an outlet link that represents the discharge - depth relationship between the surface and underground pipes. When an inlet is pressurized, the flow is reversed to the major system, and the flow travels overland to the next available inlet or ponds until the pressurized inlet becomes available to receive flow. SWMM's dual drainage is limited to one-directional flow and does not allow runoff to flow sideways, such as over a curb. Dual drainage was applied to the entire watershed using PCSWMM's Dual Drainage Creator Tool, which replicates selected inlets and downstream conduits (the minor system) with surface nodes, transects, and outlets (the major system). Submerged nodes are assigned a surcharge depth of 0.75 feet to represent the depth of the partnered node in the major system. To simplify the process, roadways were assumed to have the cross-section shown in Figure 4-13; it was understood that this assumption may limit the accurate simulation of flow if a node is pressurized.

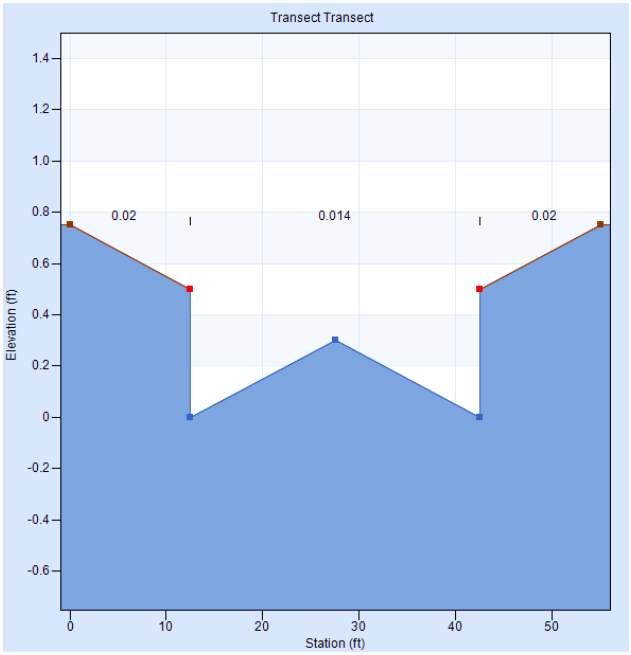

Figure 4-13. Road cross-section for dual drainage modeling of the major system.

4.6 Preliminary Application

After inputting parameter estimations, a preliminary application is necessary to audit the model and identify errors. The model was tested on Howard County's 10-year SCS Type II 24-hour storm, which is equivalent to 4.91 inches of total rainfall. The model produces an inflow (cfs) hydrograph for the outfall (Figure 4-14), and tracks flows and states (e.g., depth) in every link and node of the model. The auditing of the model identified missing depths for nodes, negative slopes, and inconsistent flooding in nodes. A node's depth is calculated by taking the difference between the rim

elevation and the invert elevation; thus, missing depths were due to either missing invert elevation or rim elevation. Rim elevation was estimated with the local DEM

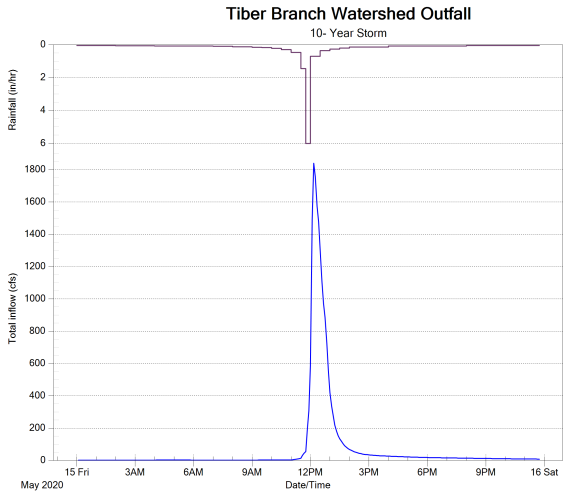

Figure 4-14. Rainfall hyetograph and outfall hydrograph for Howard County's 10-year storm.

layer, and the invert elevation was estimated by nearby invert elevation.

Because the watershed contains no pumps to move water uphill, all conduits in this model should have a positive slope and work with gravitational forces to move runoff through the stormwater network. Negative slopes identified in the audit were caused by inaccuracies of inlet and outlet offsets; in some cases, the outlet offset was lower than the inlet offset. This caused the flow to travel upward rather than downward, as shown in Figure 4-15, where J1 and J2 denote the nodes, H1 is the outlet offset, and H2 is the inlet offset. If H1 is 0.1 ft and H2 is 0.2ft, the flow will travel upward from J1 to J2 causing a negative slope. H1 can be adjusted to be greater than H2 or H2 less than H1 causing the flow to travel downward. If a negative slope occurred in a conduit, the offsets were estimated to be flush with the invert of the connecting

nodes. This assumption may not be valid for all conduits, but the negative slope error was corrected.

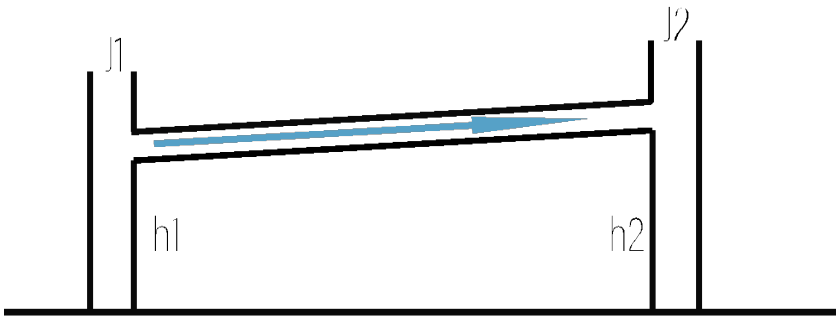

Figure 4-15. Diagram showing a negative slope caused by offsets.

After a simulation, PCSWMM provides flooding, routing, and runoff status for the model. The flooding status classifies nodes that have flooded. These nodes were analyzed to ensure they were flooding under the right conditions. Due to the link and node assembly, when creating tributaries as explained in section 4.4.2, added stream nodes were often flooded because the maximum depth did not match the depth of connected links. Changing the maximum depth of these nodes for added tributaries reduced the number of nodes flooding. The flooding status also identified nodes that were flooding because the conduit dimensions downstream were smaller than the upstream dimensions. Adjusting the downstream conduits' dimensions to agree with the surrounding dimensions further reduced the number of flooded nodes. At this point, the model was ready for a continuous or event simulation. Figure 4-17 displays the

model for the entire watershed, but some features are not shown due to the amount of detail. The yellow circle in Figure 4-16 is the location of the Timberland Circle community. The zoomed-in map (Figure 4-17) displays the complexities of the system. Overland flow is calculated for each subcatchment and the input is assigned to the designated junction. The precipitation flows through the conduits (black lines) until it reaches the storage node (green box). The storage curve denotes the volume of the storage pond and the weirs and orifices (orange and pink lines) regulate the flow to the nearby tributary (green lines) where it connects to the stream network (blue lines). The storage node has two weirs, one for flow through the riser and the other for the emergency spillway, represented as separate links in the diagram. Except for the natural stream, the links in Figure 4-17 are schematic; they do not follow the exact paths of pipes or surface flow in this locality. In each case, the length parameter assigned to each link represents its actual physical flow length.

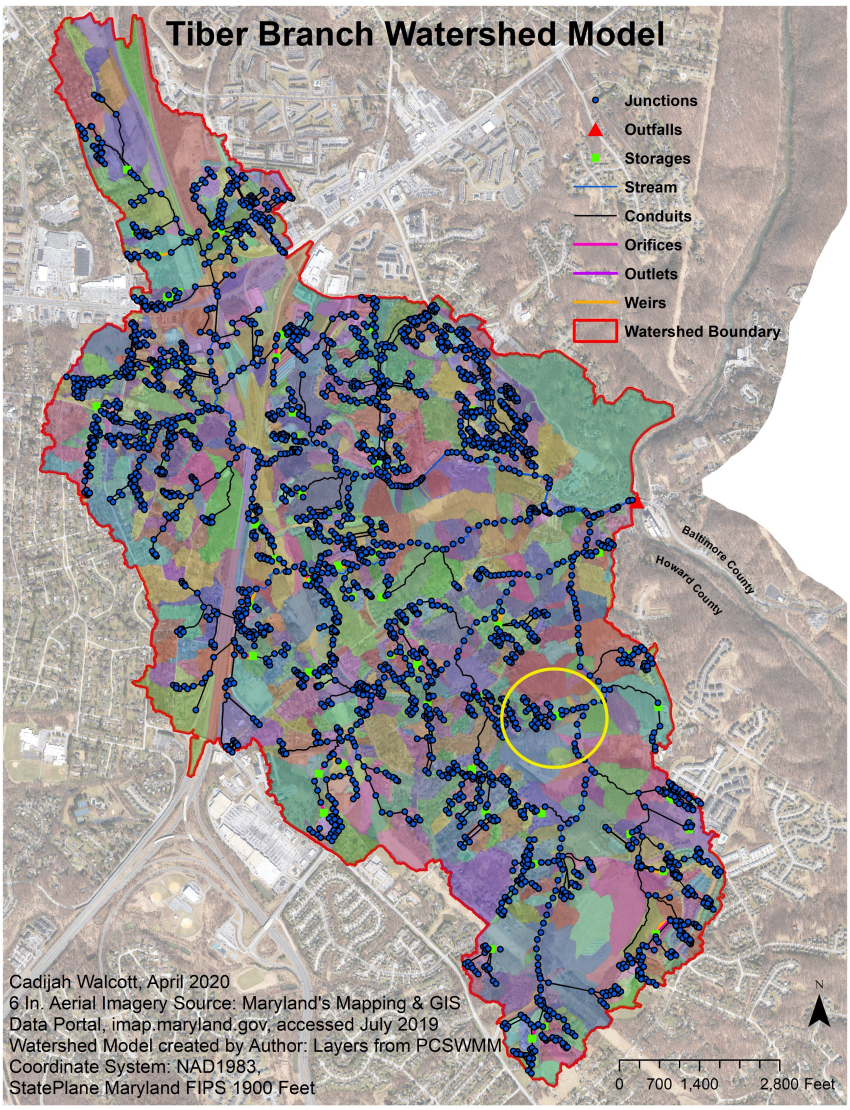

Figure 4-16. SWMM model for Tiber Branch Watershed.

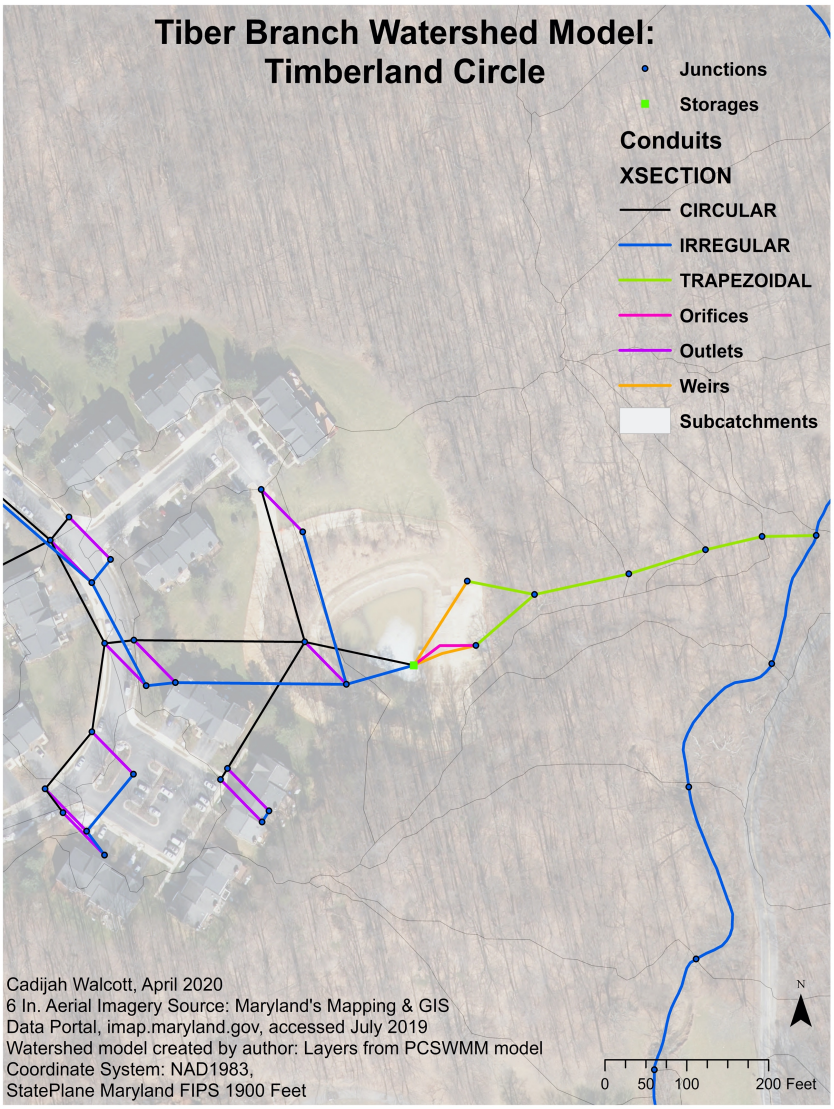

Figure 4-17. Timberland Circle neighborhood of Tiber Branch Watershed.

Chapter 5. Calibration

The model is a system representation of the processes in the TBW. Phase One of the modeling process was to collect the data, input parameter estimates that come from the watershed characteristics, and input observed data from the rain gage, all coming with some margin of error. Phase One ends with the preliminary application of the model to identify errors and ensure the model can simulate results. Phase Two of the modeling process includes calibration and validation. Calibration is a cyclical process evaluating and adjusting parameter estimates from Phase One by comparing the simulated data to observed data. The validation process uses independent input and observed data to confirm that the adjustments made in the calibration step are accurate and able to simulate observations that were not used in the calibration.

5.1 PCSWMM's Sensitivity Based Radio Tuning Calibration

PCSWMM's Sensitivity Based Radio Tuning Calibration (SRTC) tool was used for the calibration- related steps in this study. Parameter estimates come with varying ranges of uncertainty; Table 5-1 shows the criteria used to rank the uncertainty associated with different parameters. Table 5-2 lists the SWMM parameters with their ranking and uncertainty ranges. The SRTC uses the uncertainty ranges to calculate sensitivity points for the parameters. The sensitivity points consist of the minimum, maximum, and original values, as well as a value halfway between the original and maximum and the original and minimum. The SRTC tool performs parameter sensitivity and calibration calculations at specific locations (objects) in the model that correspond to the locations of the observed data.

Table 5-1. Uncertainty categories and ranges used for parameters in calibration process.

Category	Category Description	Uncertainty Range (%)
B	Completely correct or completely incorrect	Null/Complete
1	Can be measured with almost total certainty	5-10
2	Can be estimated with a high degree of certainty in the field, design office, or lab	10-25
3	Cannot be easily measured in the field or lab	25-50
4	Cannot be measured with any certainty at all	50-100

Source: (James, 2005)

The SRTC tool outputs various analyses to choose from to evaluate the model's performance. One option is a graph displaying the observed, simulated, and calibrated time series. PCSWMM's SRTC uses the term "calibrated" in this context to refer to the simulated time series that results when a parameter is changed by adjusting the radio-tuning tab. Furthermore, the tool produces a sensitivity ranking of the parameters by displaying the changes in the simulation output (for example, water depth or one or more Goodness of Fit [GOF] statistics, discussed below) based on changes in the parameters. Sensitivity analysis determines the parameter's influence on the simulation. If the parameter does not cause the simulated value to change positively or negatively, the model is not sensitive to that parameter. This information is useful because it makes the modeler aware of how much effort they should invest in that parameter's estimation.

Table 5-2. Parameters estimated in the model with the corresponding uncertainty ranking and range.

Category	Input Parameter	Uncertainty Range (%)
	Junction	
1	Invert Elevation	5-10
1	Rim Elevation	5-10
1	Depth	5-10
1	Ponded Area	5-10
	Storage	
1	Invert Elevation	5-10
1	Rim Elevation	5-10
1	Depth	5-10
2	Initial Depth	10-25
	Conduit	
1	Inlet offset	5-10
1	Outlet Offset	5-10
	Outlet	
1	Invert Elevation	5-10
2	Coefficient	10-25
2	Exponent	10-25
	Orifice	
1	Height	5-10
1	Width	5-10
1	Invert Elevation	5-10
1	Discharge Coefficient	5-10
	Weir	
1	Height	5-10
1	Length	5-10
1	Side Slope	5-10
1	Inlet Offset	5-10
1	Discharge Coefficient	5-10
	Subcatchment	
4	Width	
1	Area	5-10
1	Ground Slope	5-10
2	Manning's n for Impervious	10-25
4	Manning's n for Pervious	50-100
3	Depression Storage - Impervious	25-50
4	Depression Storage - Pervious	50-100
4	Zero Impervious	50-100
2	Curve Number	10-25
2	Drying Time	10-25

Note: Created by author.

5.1.1 Goodness of Fit Statistics

PCSWMM's error function tab provides computed GOF statistical values to use to evaluate the match between the simulated results and the observed data. The error tab rapidly adjusts when parameter estimations change under the radio tuning tab or the extent of the time series is adjusted. In this study, the GOFs selected for evaluation were the coefficient of determination, the standard error of estimate, and the ratio of standard error of estimate to the standard deviation of the observed data. The coefficient of determination, R^2, is used in regression analysis to determine how well the simulated results predict the observed data. Ranging from 0 to 1, R^2 represents the proportion of observed variation that can be explained by the simulated variation. A value of one would indicate that the simulated results match the observed data perfectly, or that the model explains 100% of variation in the observations. R^2 is calculated by equation 5-1:

$$R^2 = \left(\frac{\sum\left(y_{obs}^i - \overline{y_{obs}}\right)\left(y_{sim}^i - \overline{y_{sim}}\right)}{\sqrt{\sum\left(y_{obs}^i - \overline{y_{obs}}\right)^2 \sum\left(y_{sim}^i - \overline{y_{sim}}\right)^2}} \right)^2 \qquad 5\text{-}1$$

where R^2 is the coefficient of determination (dimensionless), y_{obs} is a observed value, $\overline{y_{obs}}$ is the mean of the observed values, y_{sim} is a simulated value, and $\overline{y_{sim}}$ is the mean of the simulated values.

The standard error of estimates (SE), in units of the observed and simulated variable, measures the accuracy of the simulated results by taking the sum of the squared errors between the observed and simulated values. Smaller SE implies

simulated results are more accurate at predicting the observed value. SE is calculated by Equation 5-3:

$$SE = \sqrt{\frac{\sum\left(y_{obs}^{i} - y_{sim}^{i}\right)^{2}}{n}} \qquad 5\text{-}2$$

where y_{obs} is an observed value, y_{sim} is a simulated value, and n is the number of observation/simulation pairs.

The final statistic is a dimensionless statistic that uses SE to evaluate the model's accuracy and is calculated by:

$$\frac{SE}{Sy} = \sqrt{\frac{\sum\left(y_{obs}^{i} - y_{sim}^{i}\right)^{2}}{Sy}} \qquad 5\text{-}3$$

where *Sy* is the standard deviation of the observed data. Statistically, this value should range between 0 and 1, 1 being a poor model and 0 being an excellent model in terms of accuracy. This statistic is not provided in PCSWMM's error function tab and is calculated independently.

5.2 Hudson Branch Submodel

Evaluation of model performance requires observed data to which the model predictions can be compared. The Hudson Branch tributary of TBW has a stage gage located just upstream of the bridge crossing over the river on Frederick Road near Rogers Ave (Figure 5-1). The gage reports data typically on an hourly basis but the reporting time interval may decrease during storm events to include more detail. The Hudson Branch gage is the only gage in the TBW that could provide data for an observed time series in the calibration process. Howard County's government provided

two years of stage data for the observed time series, from January 1st, 2018 to December 31st, 2019, including hour-minute-second time and stage in feet. PCSWMM

Figure 5-1. Stage gage for data used in sensitivity/calibration process. Located on Hudson Branch tributary by Ellicott City Colored School House bridge.

does not shift between standard time and daylight-saving time; therefore, it was necessary to adjust the observed data to Eastern Standard Time, so that observed and computed data lined up.

Additionally, the PCSWMM model of TBW was not set up to include a groundwater compartment that would have generated baseflow; hence the observed data was altered to remove an estimated baseflow and include only direct runoff. In performing baseflow separation on the observed depth time series, baseflow was extracted by linear interpolation between the beginning depth and ending depth of the

selected event. This approach allowed baseflow separation on a rainfall-runoff event basis and not on the entire series. The baseflow was removed from the total runoff to obtain a time series of observed direct runoff to compare to the simulated direct runoff (Figure 5-2).

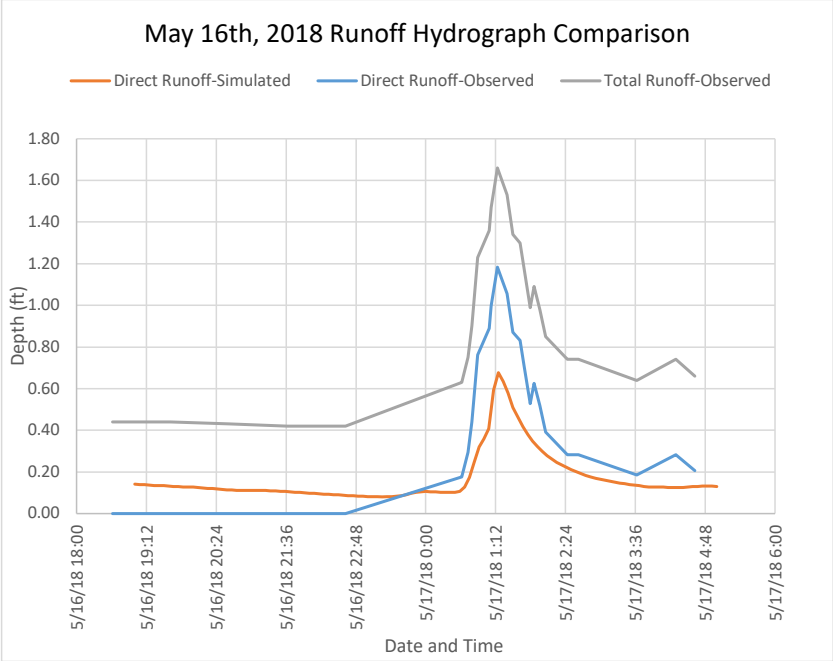

Figure 5-2. Hydrographs comparing the results of baseflow separation from the observed data to the simulated data.

The model for TBW is quite comprehensive, and the computational run time is very long due to the size and extensive detail. Because the location of the observed data is not at the outlet, but along the Hudson Branch tributary, a Hudson Branch submodel was created for Phase Two. The watershed for the submodel is approximately 34% of the TBW model by area, and the model's link CJ5671 corresponds to observed time series at the Hudson Branch gage.

Graphical analysis and statistical tests are used as evaluation criteria during the parameter sensitivity and calibration process. The graphical analysis allows a preliminary assessment of the model performance and helps the user interpret the statistical tests. SRTC tool results include a time series plot of the observed and simulated data, as well as scatter plots displaying the maximum depth for observed and simulated events along a 45-degree line to test the linearity between the data. If the data lie along the line, there is a positive relationship between predicted and observed depths. If the data falls along the line but scatters randomly or in a cluster, then there is bias in the model that should be corrected.

5.2.1 Using PCSWMM's SRTC Tool

Applying the SRTC tool to the TBW model required additional analysis in order to interpret the tools' output correctly and manipulate it into an appropriate form. The TBW model was designed to examine the impacts of flooding on the watershed. Event modeling was selected to focus on floods and to reduce the model's running time (compared to continuous simulation). From the two years of rainfall data, 43 events were selected based on duration, total rainfall, and time period. The SRTC tool was expected to provide GOFs for the specific events and then for the entire 43-event simulation run, allowing use of the radio tuning tool to adjust parameters and improve the GOF values. Since the model's simulated results only included the data from the events (with no simulated values between them) the SRTC tool was expected to calculate the error functions for the model only comparing the observed data during the selected events. In PCSWMM's summary hydrograph output (Figure 5-3), the light blue vertical lines are the locations of the specified events along the timeline. The blue

boxes (added by the author) in Figure 5-3 represent estimated periods of the time series when no events occurred. On first inspection, it was unclear whether these periods and other non-event periods were included in PCSWMM's reported GOF calculations.

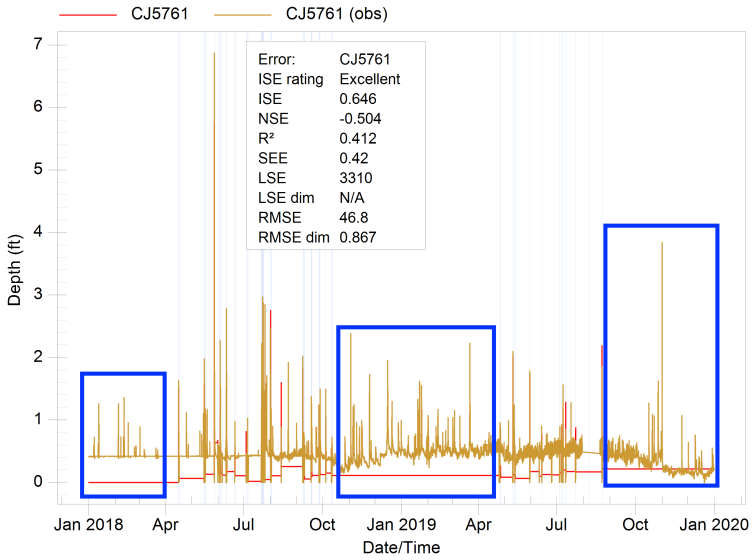

Figure 5-3. PCSWMM's hydrograph output for comparing observed and simulated data.

Unfortunately, within PCSWMM and its documentation it was unclear whether the GOFs provided for the entire extent of data (Figure 5-3) compare the observed data to the simulated data only for the specified events or for the continuous time period. Published research using the SRTC tool to calibrate models also lacked information clarifying the unknown method used by PCSWMM to give the model an overall GOF evaluation for all events rather than specific events or parameters. For example, Randall (2017) used the PCSWMM's SRTC tool to calibrate a dual drainage model for an urban area on 12 events between 2009 and 2013; that study reports GOFs used to estimate

the model parameters and suggests the GOFs are calculated based on the total and peak flow and not the entire model's hydrograph. Broekhuizen (2020) researched event selection approaches for green urban drainage systems and used the SRTC tool to calibrate the model and took the averages of GOFs for the selected events.

To analyze PCSWMM's method, MATLAB was used independently to reproduce PCSWMM's GOF values. It was assumed that the GOF values in Figure 5-3 was for the entire continuous time series and not just the events. To match the dates and times of the data, first the observed data was linearly interpolated to the simulated time points; the resulting GOFs did not match PCSWMM's values. Second, the simulated depth was linearly interpolated to the observation time points; for this experiment, most of the GOFs values matched the values in GOFs (Figure 5-3). It was concluded that the overall simulation statistics reported by PCSWMM (Figure 5-3) represent the entire time series, with the simulated results linearly interpolated to the times of the observations between the specified events. Including these inter-event periods in the GOF calculations would be misleading because the model is not being used to simulate depth during those periods. In addition, this analysis revealed that the values reported by PCSWMM for integral squared error (ISE) and root mean square error (RMSE) are multiplied by a factor of 100.

Further, the PCSWMM documentation described the RMSE and the SE as different GOFs with different equations, although statistically they are the same. According to the PCSWMM documentation (Computational Hydraulics International (CHI), 2020), The RMSE is calculated using Equation 5-4:

$$RMSE = \sum \sqrt{\frac{\left(y_{obs}^{i} - y_{sim}^{i}\right)^{2}}{n}} \qquad 5\text{-}4$$

Where RMSE has units of the variable (for example, feet), y_{obs} is an observed value, y_{sim} is a simulated value, and n is the number of observations. The summation should be of the errors and not outside of the square root. Except for the previously mentioned factor of 100, the software appears to be performing the calculation correctly, but the published equation is incorrect.

Ultimately, the goal was to adjust parameter values to calibrate the model for the 43 events only. To do this, the observed and simulated data were edited outside of PCSWMM to remove the non-event time periods. The adjusted datasets were used in MATLAB to calculate the GOFs by linearly interpolating the simulated depth to the times of the observed data (Figure 5-4). The observed data without the inter-event periods were input into PCSWMM; the resulting GOF values as estimated by the SRTC matched those determined using MATLAB. This process established the ability to calculate GOFs and experiment with parameter sensitivity for all the simulated events without contamination by non-simulated interevent periods.

Using Table 5-2 and knowledge of the estimation process, eight parameters of the TBW model were selected for analysis in the sensitivity/calibration process. The effects of varying these parameters over reasonable ranges of uncertainty were investigated graphically and numerically.

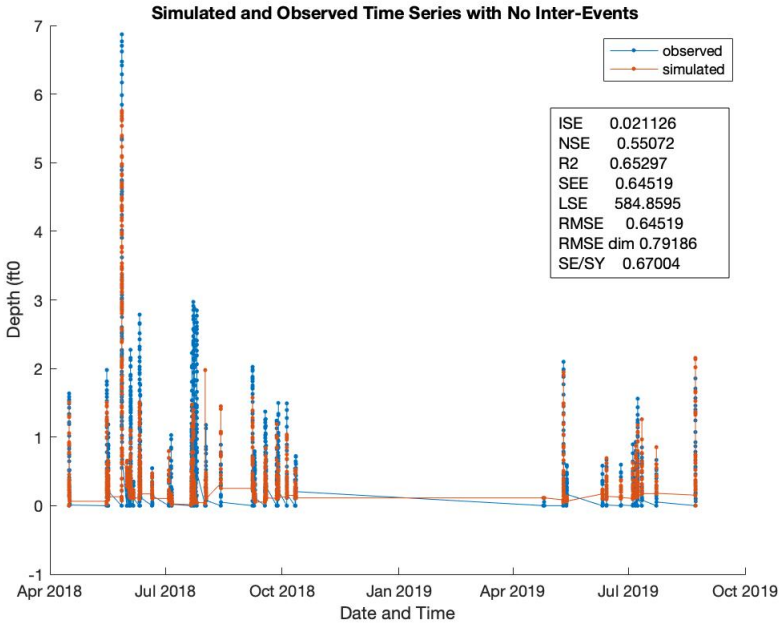

Figure 5-4. Simulated and Observed without Inter-events.

Chapter 6. Results

The essential result of this work is the successful completion of a detailed PCSWMM model of overland and stormwater conveyance flow in the Tiber Branch Watershed (Objective 1). The model runs successfully at the audit/preliminary application stage. As discussed in Chapters 4 and 5, this accomplishment represents the synthesis of numerous data sets and tools.

The model was assessed without calibration (adjusting parameter values). The overall model (only events) had a R^2 of 0.65 meaning the model is able to explain 65% of the total variation not explained by the mean. Based only on R^2, the model may be considered a *good* model (R. McCuen, personal communication, 2018) but other GOFs were checked as well. The SE/SY for the overall model is 0.67 suggesting the model has very poor accuracy in predicted the observed data. This GOF ideally should be less than 0.3 for the model to be considered excellent for use (R. McCuen, personal communication, 2018) . Goodness of fit statistics were calculated for each of the 43 simulated events (Table 6-1).

Table 6-1. 43 selected events and Goodness of Fit statistics.

Event	Beginning Date and Time	Duration (h)	Total Rainfall (in)	R^2	SE	SE/SY
1	4/15/18 22:00	16	1.68	0.88	0.32	0.61
2	5/15/18 16:00	10	1.32	0.77	0.44	0.69
3	5/16/18 19:00	10	0.8	0.90	0.27	0.76
4	5/27/18 11:00	10	7.52	0.65	1.08	0.62
5	5/31/18 14:00	10	0.4	0.09	0.28	1.40
6	6/2/18 11:00	14	0.4	0.24	0.16	0.99
7	6/3/18 8:00	14	2.16	0.73	0.82	1.38
8	6/5/18 15:00	8	0.4	0.74	0.10	0.70

9	6/10/18 10:55	9	1.32	0.89	0.64	0.75
10	6/11/18 0:30	7.67	0.88	0.91	0.51	1.01
11	6/20/18 10:40	11	0.52	0.62	0.38	2.40
12	7/3/18 16:30	10	0.44	0.64	0.15	0.88
13	7/5/18 12:25	9	0.32	0.34	0.39	1.14
14	7/6/18 0:00	8	0.2	0.04	0.09	1.07
15	7/21/18 6:25	24	3.8	0.71	0.57	1.09
16	7/22/18 12:55	18	1.92	0.49	1.02	1.03
17	7/23/18 18:20	27	2.52	0.07	1.01	1.27
18	8/1/18 7:10	5	1.08	0.00	0.52	92.84[2]
19	8/1/18 19:00	10	0.48	0.59	0.30	0.87
20	8/13/18 15:15	3.75	1.08	0.60	0.36	1.31
21	9/7/18 15:45	7.25	1.64	0.76	0.58	0.83
22	9/8/18 10:55	10	0.44	0.15	0.19	0.97
23	9/8/18 21:00	24	2.04	0.52	0.33	1.61
24	9/17/18 9:55	27.08	1.56	0.84	0.36	1.01
25	9/26/18 16:20	5	0.72	0.87	0.23	0.56
26	9/27/18 10:05	19	1.64	0.72	0.43	1.24
27	10/4/18 16:30	6	0.6	0.97	0.19	0.43
28	10/11/18 4:00	6	0.36	0.72	0.10	0.53
29	10/11/18 14:25	10	0.84	0.27	0.25	1.21
30	4/25/19 22:25	5.75	0.24	0.48	0.61	-[3]
31	4/26/19 13:15	5	0.16	0.65	0.56	2.54
32	5/10/19 14:50	13	1.04	0.91	0.29	0.42
33	5/12/19 23:35	16.08	0.68	0.01	0.23	1.37
34	5/30/19 13:30	6	0.84	0.90	0.18	0.33
35	6/10/19 11:25	5	0.32	0.63	0.15	0.83
36	6/13/19 16:00	5	0.32	0.79	0.10	0.44
37	6/24/19 23:00	6	0.4	0.86	0.12	0.57
38	7/4/19 10:25	4.33	0.52	0.80	0.15	0.55
39	7/6/19 18:00	5	0.64	0.72	0.17	0.60
40	7/8/19 4:50	6	1.28	0.82	0.34	0.68
41	7/11/19 13:00	6	0.64	0.78	0.15	0.55
42	7/23/19 0:20	4	0.52	0.92	0.10	0.45
43	8/22/19 17:35	7.5	1.56	0.90	0.21	0.35

[2] The standard deviation is very small (thousandth place) because most of the depths for this event are 0.

[3] The standard deviation is 0. There was no observed direct runoff at this location.

Event 34 (Figure 6-1) and event 43 (Figure 6-2) are considered the best event simulations based on their calculated R^2 (0.90 for both) and SE/SY(0.33 and 0.35, respectively). Event 34 hydrograph's rise and recession, and magnitude of depth closely match the observed data reducing the SE and indicating good model accuracy.

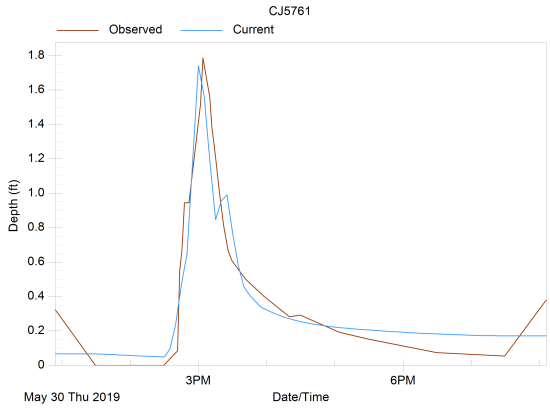

Figure 6-1. Top event for the model with R^2 = 0.90 and SE/SY = 0.33.

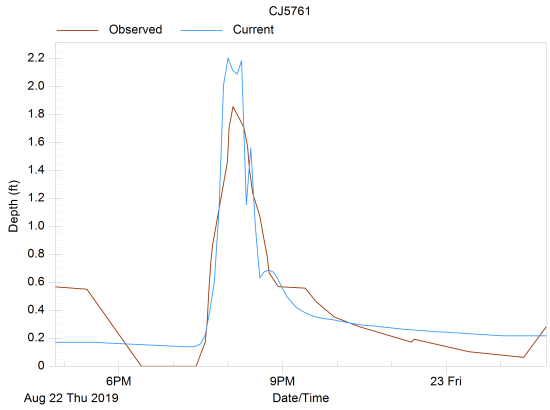

Figure 6-2. Another top event for the model with R^2 = 0.90 and SE/SY = 0.35.

In event 43, the model is able to accurately time the peak and shape of the hydrograph but overestimates the peak for the event.

May 27th, 2018 was the second flash flood to hit Ellicott City in the last four years with 7.52 inches of rainfall reported at the rain gage (Figure 6-3). This is the largest rain event in the model. The model does well at lining up the timing of the simulated peaks to the observed data but falters on the matching the magnitude of the observed data.

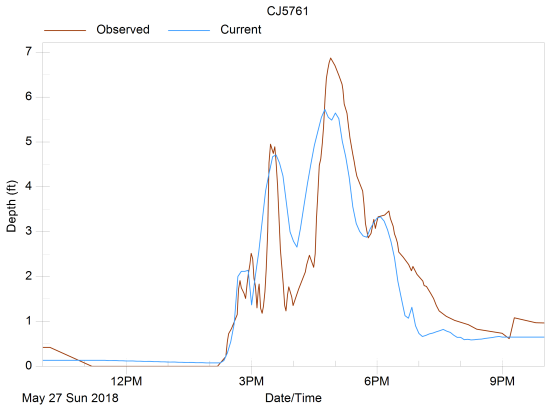

Figure 6-3. Largest event in terms of total rainfall and receives R2 = 0.65 and SE/SY = 0.62.

After reviewing all the events, it was clear the model was able to produce the timing of hydrograph rise, recession, and peak as the observed data but lacked the same accuracy in predicting the maximum depths. On July 23rd, 2018, the model responded to rain at the rain gage but struggled with producing any noticeable change in depth in the stream (Figure 6-4). This occurred in 9 out of the 43 events, implying that model relies heavily on precipitation data to accurately predict depth in the stream. The rain gage used is located on the eastern border of the watershed; if precipitation falls

elsewhere in the watershed the model will not be able to accurately calculate the runoff amounts for each subcatchment. Radar rainfall from the July 23rd event confirms rainfall in other regions of the watershed and not at the rain gage (Figure 6-5) (T. Gleason, personal communication, 2020). The precipitation input appears to be the defining quantity for accuracy of predicted depth at the Hudson Branch gage; it is not appropriate to tune parameters to compensate for nonrepresentative rainfall. Therefore, the model wasn't calibrated because the precipitation data used was not representative of the entire watershed. Chapter 7 discusses other possibilities to correct this error.

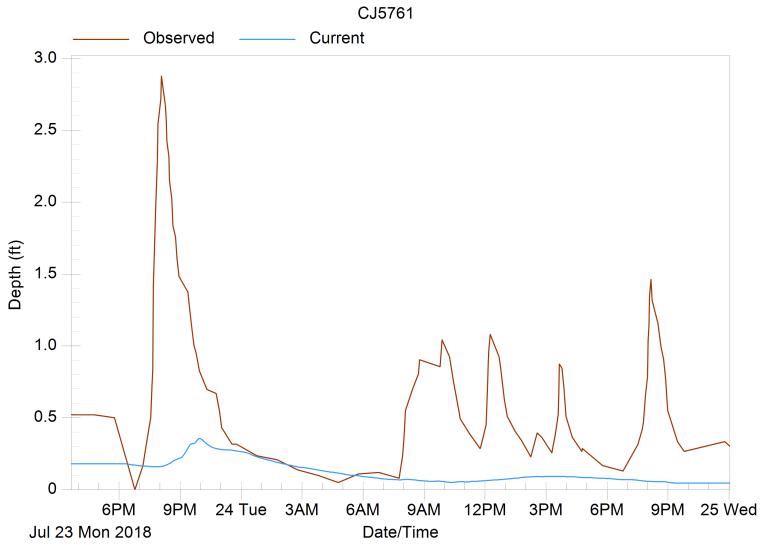

Figure 6-4. Very small response to rainfall compared to observed data.

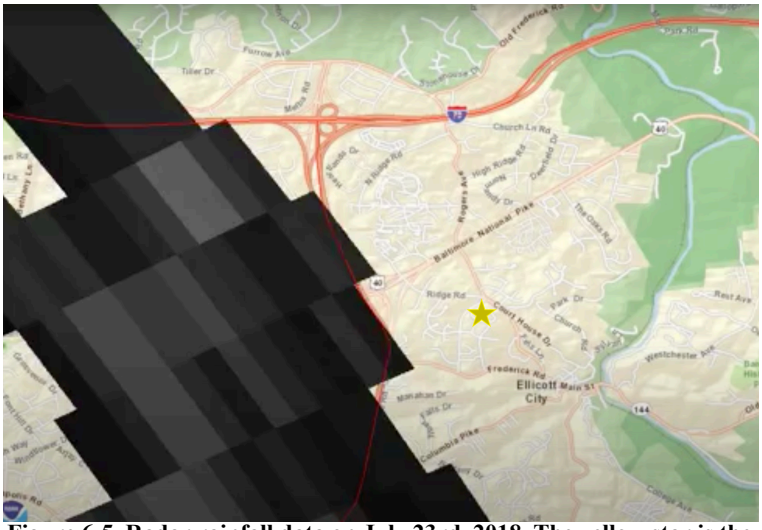

Figure 6-5. Radar rainfall data on July 23rd, 2018. The yellow star is the location of the rain gage used in the model.

Figure 6-6 displays an event that did not reflect the conditions of the watershed. The observed data shows there is no direct runoff for the selected time period, but the inputted data showed rain at the gage, therefore the model computed runoff. This is another example of the selected rain gage not being representative of the watershed.

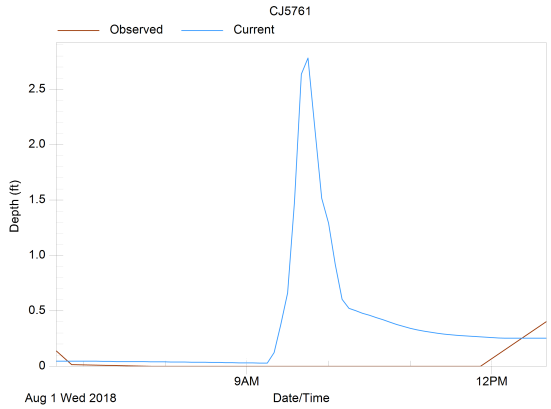

Figure 6-6. Model computes runoff for an event not detected by the observed data.

The calibration and validation process were not completed on the model but the SRTC tool could still be applied for sensitivity analysis (Objective 2). A multitude of parameters for various SWMM objects could be selected for a sensitivity analysis. The parameters used to test sensitivity in the model were selected based on high ranking of uncertainty and the access to data used to estimate the parameters. Eight parameters were selected to reduce run time.

The SRTC tool provides two graphical plots to examine parameter sensitivity: Ranked Sensitivity Graph (Figure 6-7) and Sensitivity Gradient Graph (Figure 6-8) The ranked sensitivity graph ranks the parameters based on the range of depth for link CJ5671 divided by the depth with no parameter adjustment (mean normalized sensitivity) (CHI, 2020). The sensitivity gradient graph displays the change in depth with a percent change within the uncertainty range selected for each parameter for the specific link CJ5761 in the model. The eight selected parameters show sensitivity in

the model with the CN parameter displaying the most sensitivity. The CN and percent of impervious are the two most sensitive parameters of the 8 selected.

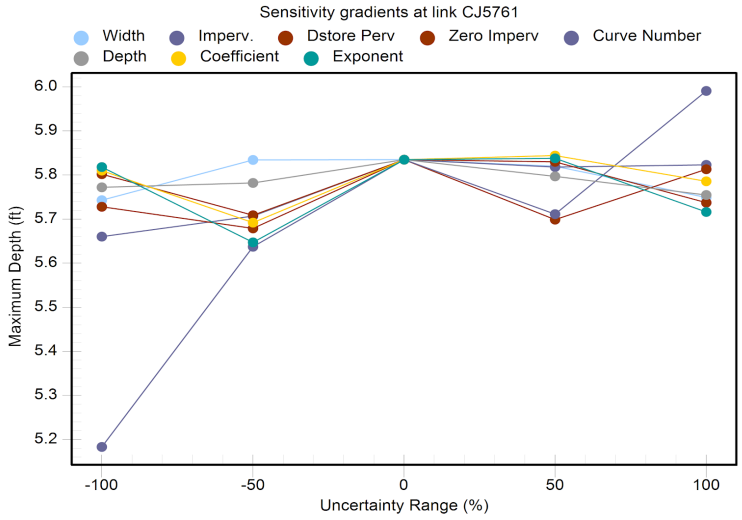

Figure 6-7. Sensitivity plot for selected parameters at link CJ5761.

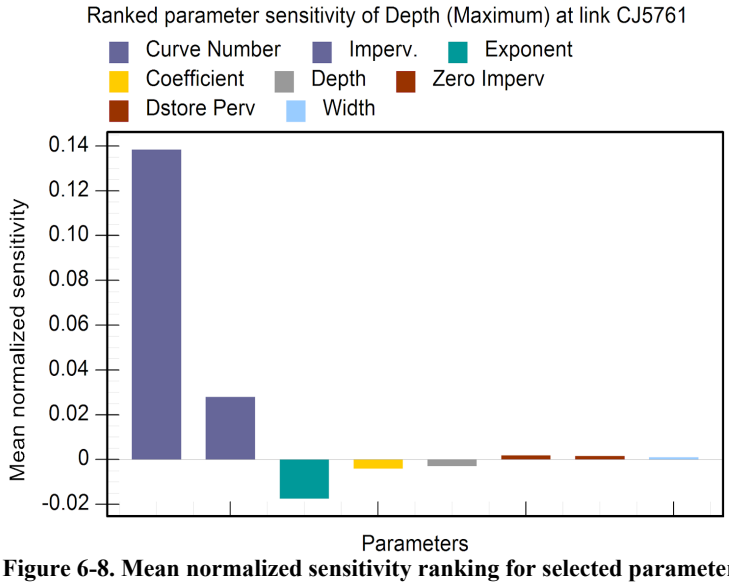

Figure 6-8. Mean normalized sensitivity ranking for selected parameters.

Curve number and percent of imperviousness sensitivities were assessed using events 9 and 27. Without calibration, both events were able to match the timing of the peak and the shape of the hydrograph but not the magnitude of the depth. The parameters were adjusted using the radio tuning tab in the SRTC tool; these adjustments increased the maximum depth and at the same time decreased the standard error of estimate, indicating improved model accuracy.

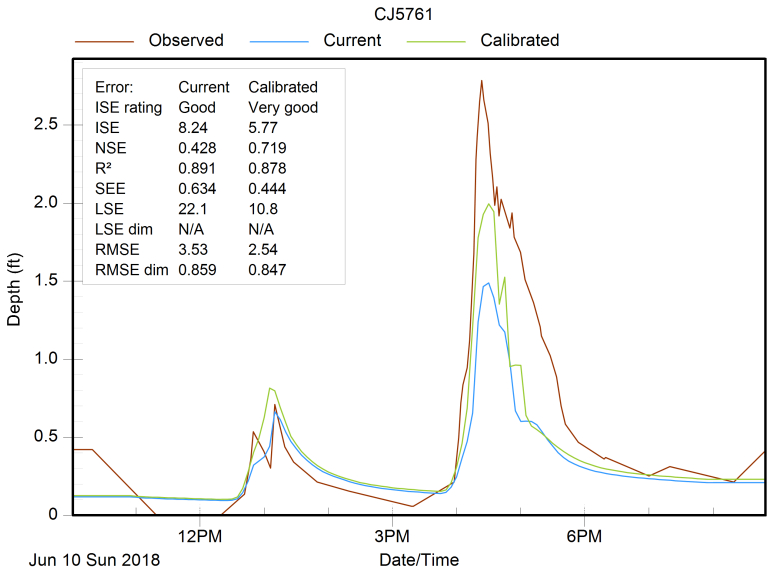

Figure 6-9. Event 9 sensitivity to parameter adjustments.

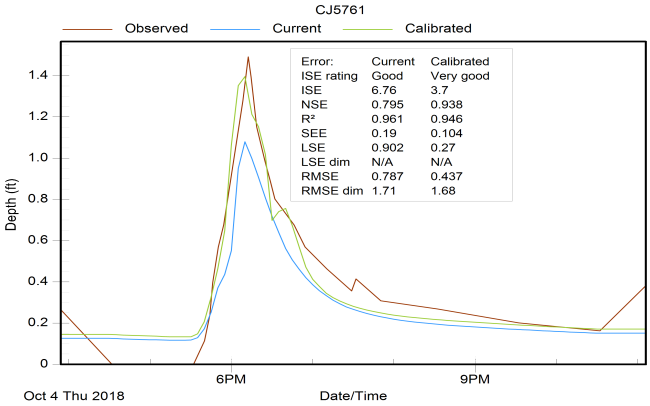

Figure 6-10. Event 27 sensitivity to parameter adjustments.

A stormwater detention pond within the watershed is utilized during the May 2018 flash flood in Ellicott City and produces a hydrograph (Figure 6-11). The pond has a maximum depth of 9.68 feet and is equipped with a multistage riser and a low flow orifice. The model simulated results for the single event, therefore the pond's initial depth is 0 feet at the beginning. The maximum water level during this event is 9.28 feet and declines to 4.5 feet at the end of the event by using the weirs and orifices.

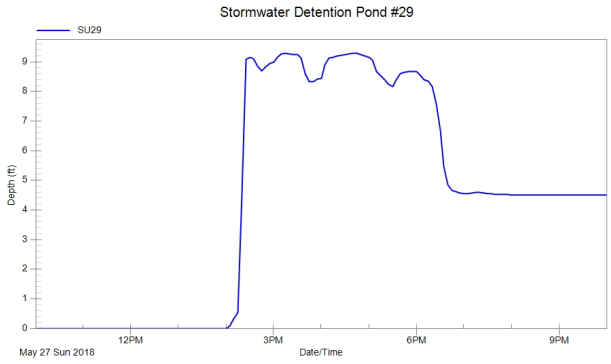

Figure 6-11. Depth hydrograph for wet stormwater detention pond in TBW.

Study Objectives 3, 4, and 5 (Detail challenges with creating an extensive model for a large urban watershed; identify data needs for the calibration and validation phases of model development; and provide suggestions for application of the model to investigate the potential of LID to reduce urban flooding in the TBW) are addressed in the Conclusion and Discussion (Chapter 7).

Chapter 7. Conclusions and Discussion

Aging and crumbling stormwater networks built for past weather patterns are an ongoing challenge for stormwater divisions. Repairs are costly and state and local governments are often left to cover the cost. Coupled with inadequate performance, the stormwater networks leave many communities underwater exacerbating their vulnerabilities. This research has created a model of the Tiber Branch Watershed that can be applied in future investigations of urban flooding in Ellicott City, Maryland. The lessons learned in this process can guide future work developing a model in SWMM/PCSWMM format for similar urban locations.

7.1 Research Overview

This thesis aimed to detail the processes used to create a physically explicit model of the Tiber Branch watershed. Chapter 4 discusses Phase One and the process of developing the model and the different compartments of a SWMM model (Objective 1). Datasets from multiple sources were used with GIS and PCSWMM tools to reformat for the model's needs. The resulting model consisted of 1,359 subcatchments, totaling 2434.8 acres and tens of thousands of objects. Chapter 5 discusses Phase Two, the challenges faced with using PCSWMM's built-in calibration tool, and the use of PCSWMM's built-in parameter tool to explore the model's sensitivity to uncertain parameters (Objective 2). In the end the model was not calibrated due to lack of representative rainfall for the entire watershed.

The experience of developing the TBW model provides insight on the process of modeling urban watersheds (Objective 3). A comprehensive watershed model takes time to design and will fluctuate based on users' capabilities and available datasets; this should be noted before taking on the endeavor. Many challenges were faced while putting together this model; most arose from datasets. Although extremely detailed, the dataset documenting the stormwater network was incomplete and estimates were needed to fill in missing values. A large region of the watershed did not have mapped data on the stormwater network, causing uneven subcatchment sizes and likely reducing the accuracy of runoff values. In a flood event, stormwater detention ponds are used to hold water to a certain threshold and storage curves were estimated to determine a pond's geometric shape and capacity within the model. Local DEM and aerial imagery layers and GIS tools were necessary in creating the model.

The TBW model results illustrate the need for more detailed precipitation data (Objective 4). Storms are often localized and may occur in a watershed and not at the rain gage located near the watershed, or vice versa. This occurred in this model with only one source of precipitation data and the assumption that rainfall was equally distributed throughout the watershed was proven false. PCSWMM offers the ability to input multiple rain gages and import radar rainfall data to accurately represent spatial variation of rainfall in the watershed. These options should be considered to move forward with the calibration process.

An accurate, detailed urban model can allow communities to perform virtual experiments with possible solutions to flooding (Objective 5) . For example, LID storage could be added, similar to the stormwater ponds already included in the model.

The overall effects of many such structures could be assessed in a physically detailed fashion, without assumptions or empirical coefficients. Communities can test sizing of stormwater inlets and conduits to determine if the quantity of runoff in flooding areas will decrease. For example, rain barrels are low cost LIDs used to capture rain where it falls and stores it for later use and a watershed model can determine if a certain portion of the community were to use rain barrel how much will runoff decrease.

7.2 Discussion

After the 2018 flash flood event in Ellicott City, FEMA awarded the state of Maryland over $1 million for flood prevention in the historic city and Howard County gave an additional $400,000 to the fund (Murillo, 2018). This enabled the county to hire contracting services from companies, such as McCormick and Taylor, to analyze different watersheds and give suggestions on improvement of flooding issues. Unfortunately, not all communities are offered the same incentives to reduce flooding risk. Fortunately, watershed models can be developed free with SWMM or users can pay $1440-$2160 annually for a user-friendly experience and valuable support system with CHI's PCSWMM. These software tools give hope to communities that are underfunded and not noticed. A community unable to contract out assignments can create their own model of varying size and complexities to work on.

This model was completed using a Windows laptop with limited disk space and memory and there were often issues with computational run time and productivity due to computer storage. According to PCSWMM documentation, minimum requirements include Windows 7 or greater, memory of at least 4 GBs and disk space of at least 2 GB (Computational Hydraulics International (CHI), 2020). A faster processor,

maximum memory and storage will improve productivity and reduce issues with the model running. The complexity of the model will also affect computational run time, the use of submodels can reduce time and the changes are transferable to the overall model.

The TBW model is a work in progress and additional steps can be taken to improve the model in the future. Ellicott City is a heavily researched area and this research can be expanded. Expansion can include inputting new information on improved portions of the stormwater network, testing recommendations proposed by contractors, and trying small scale low impact development projects to estimate a decrease in flooding.

References Cited

Ahiablame, L., & Shakya, R. (2016, April 15). Modeling flood reduction effects of low impact development at a watershed scale. *Journal of Environmental Management, 171*, 81-91.

Akhter, M. S., & Hewa, G. A. (2016). The Use of PCSWMM for Assessing the Impacts of Land Use Changes on Hydrological Responses and Performance of WSUD in Managing the Impacts at Myponga Catchment, South Australia. *Water, 8*(11).

Broekhuizen, I., Leonhardt, G., Marsalek, J., & Viklander, M. (2020). Event selection and two-stage approach for calibrating models of green urban drainage systems. *Hydrology and Earth System Sciences, 24*(2), 869-885.

Computational Hydraulics International (CHI). (2020). *PCSWMM Support*. Retrieved from Error functions: https://support.chiwater.com/79652/error-functions

Computational Hydraulics International (CHI). (2020). *PCSWMM Support*. Retrieved from SRTC: https://support.chiwater.com/78922/srtc

Computational Hydraulics International (CHI). (n.d.). *Introduction*. Retrieved from https://www.chiwater.com/Home/About#introduction

David J. Nowak, J. T. (2005, December). Projected Urban Growth (2000 – 2050) and Its Estimated Impact on the US Forest Resource. *Journal of Forestry*.

Environmental Protection Agency (EPA). (2020). Storm Water Management Model (SWMM).

Federal Highway Administration (FHA). (2013). *Urban Drainage Design Manual.* U.S. Department of Transportation. Retrieved from https://www.fhwa.dot.gov/engineering/hydraulics/pubs/10009/10009.pdf

Howard County Department of Public Works (HC DPW). (2020, Feb). Retrieved 02 2020, from Howard County Design Manual – Storm Drainage: https://www.howardcountymd.gov/LinkClick.aspx?fileticket=8bP4DgfQiKw%3d&portalid=0&timestamp=1582752086796

Howard County Department of Public Works (HC DPW). (2018). *2018 Flood Mitigation Plan Update.* Stormwater Management Division.

Howard County Department of Public Works (HC DPW). (2019). *Tiber Branch Watershed: Stormwater Retrofit Study.* Stormwater Management Division. Retrieved from https://www.howardcountymd.gov/LinkClick.aspx?fileticket=SeKdpy3CWGk%3d&portalid=0&timestamp=1561669976225

Illinois Department of Natural Resources (IDNR). (2015). *Report for the Urban Flooding Awareness Act.* State of Illinois.

James, W. (2005). *Rules for Responsible Responsible Modeling.* CHI.

Kreibich, H., Schwarze, R., Thicken, A., & Merz, B. (2010). Assessment of Economic Flood Damage. *Natural Hazards and Earth System Sciences*.

Liwanag, F., Mostrales, D. S., Ignacio, M. T., & Orejudos, J. N. (2018). Flood Modeling Using GIS and PCSWMM. *Engineering Journal, 22*(3).

Maryland Department of the Environment (MDE). (2020). *DFIRM Outreach: Flood Risk Application*. Retrieved 2019, from Flood Insurance Rate Maps: https://mdfloodmaps.net

McCormick & Taylor. (2017). *Ellicott City Hydrology/Hydraulic Study and Concept Mitigation Analysis.*

MD iMap; Maryland's Mapping & GIS Data Portal. (2020). *Data*. Retrieved 2019, from Maryland's Mapping & GIS Data Portal: https://imap.maryland.gov/Pages/data.aspx

Minnesota Pollution Control Agency (MPCA). (2020). *Available Stormwater Models and Selecting A Model*. Retrieved December 2019, from Minnesota Stormwater Manual: https://stormwater.pca.state.mn.us/index.php/Available_stormwater_models_and_selecting_a_model

Minnesota Pollution Control Agency. (2020, April). *Introduction to Stormwater Modeling*. Retrieved December 2019, from Minnesota Stormwater Manual: https://stormwater.pca.state.mn.us/index.php/Introduction_to_stormwater_modeling

Moftakhari, H. R., AghaKouchak, A., Sanders, B. F., Allaire, M., & Matthew, R. A. (2018). What Is Nuisance Flooding? Defining and Monitoring an Emerging Challenge. *Water Resources Research, 54*, 4218–4227.

Moghadas, S., Leonhardt, G., Marsalek, J., & Viklander, M. (2018). Modeling Urban Runoff from Rain-on-Snow Events with the U.S. EPA SWMM Model for Current and Future Climate Scenarios. *Journal of Cold Regions Engineering, 32*.

Murillo, M. (2018, May). *FEMA awards Md. over $1 million for Ellicott City flood-prevention efforts*. Retrieved from https://wtop.com/howard-county/2018/05/new-fema-funding-flood-prevention-ellicott-city/

National Oceanic and Atmospheric Administration (NOAA). (n.d.). *National Centers for Environmental Information.* Retrieved from GHCN (Global Historical Climatology Network) – Daily Documentation: https://www1.ncdc.noaa.gov/pub/data/cdo/documentation/GHCND_documentation.pdf

National Oceanic and Atmospheric Adminstration (NOAA). (2018, July 02). *National Weather Service*. Retrieved October 2019, from May 27th, 2018 Flooding - Ellicott City & Catonsville, MD: https://www.weather.gov/lwx/EllicottCityFlood2018

National Weather Service (NWS). (2016). *Ellicott City Historic Rain and Flash Flood - July 30, 2016.* National Oceanic and Atmospheric Adminstration.

National Weather Service (NWS). (2018). *May 27th, 2018 Flooding - Ellicott City & Catonsville, MD.* National Oceanic and Atmospheric Adminstration.

NOAA National Centers for Environmental Information (NCEI). (2019). *U.S. Billion-Dollar Weather and Climate Disasters.* Retrieved from https://www.ncdc.noaa.gov/billions/

NOAA Office for Coastal Management (NOAA OCM). (2020). *Adapting Stormwater Management for Coastal Floods.* Retrieved from Analyze Stormwater Systems: https://coast.noaa.gov/stormwater-floods/analyze/

Randall, M., Perera, N., Gupta, N., & Ahmad, M. (2017). Development and Calibration of a Dual Drainage Model for the Cooksville Creek Watershed, Canada. *Journal of Water Management Modeling, 25*.

Rossman, Lewis A.; Huber, Wayne C.;U.S. Environmental Protection Agency. (2016). *Storm Water Management Model Reference Manual: Volume I – Hydrology (Revised).* Office of Research and Development, National Risk Management Laboratory.

Runkle, J., Kunkel, K. E., Easterling, D., Stewart, B. C., Champion, S., Frankson, R., & Sweet, W. (2017). *Maryland State Climate Summary.* NOAA Technical Report .

Schurman, V. (2012, March 1). *Martha Ellicott Tyson*. Retrieved April 2020, from Friends Journal: https://www.friendsjournal.org/feat-m11-160-virginia-schurman-martha-ellicott-tyson/

Stover, J. F. (1987). *History of the Baltimore and Ohio Railroad.* Purdue University Press.

The Baltimore Sun. (1960, August 7). New Shop Center on Route 40.

Tyson, M. E. (1871). *A Brief Account of the Settlement of Ellicott's Mills, with Fragments of History therewith Connected.* Baltimore, Maryland , USA: John Murphy & Co.

U.S. Census Bureau. (n.d.). *Ellicott City CDP, Maryland*. Retrieved from Explore Census Data: https://data.census.gov/cedsci/

U.S. Department of Agriculture (USDA). (1986). *Urban Hydrology for Small Watersheds.* Technical Release 55, Natural Resources Conservation Service, Conservation Engineering Division.

U.S. Department of Agriculture (USDA). (2003). *Soil Survey of Howard County, Maryland.* Natural Resources Conservation Service, Maryland Agricultural Experiment Station (University of Maryland), Maryland Department of Agriculture, Howard County Board of Commissioners, and Howard County Soil Conservation District.

U.S. Department of Agriculture (USDA). (2007). *Chapter 7: Hydrologic Soil Groups.* Natural Resources Conservation Service.

U.S. Department of Agriculture (USDA). (n.d.). *Soil Survey Technical Note 6*. Retrieved from Natural Resources Conservation Service Soils: https://www.nrcs.usda.gov/wps/portal/nrcs/detail/soils/ref/?cid=nrcs142p2_053573

U.S. Department of Commerce, Bureau of the Census. (1982, February). Characteristics of the Population, Number of Inhabitants, Maryland. *1980 Census of Population* , 22-12. Retrieved from 1980 Census of Population: https://www2.census.gov/prod2/decennial/documents/1980a_mdABC-01.pdf

U.S. Department of Commerce, Bureau of the Census. (1992). *1990 Census of Population.* Retrieved from https://www2.census.gov/library/publications/decennial/1990/cp-1/cp-1-22.pdf

United Nations . (2018, May). *68% of the World Population Projected to Live in Urban Areas by 2050, says UN*. Retrieved from Department of Economic and Social Affairs:

https://www.un.org/development/desa/en/news/population/2018-revision-of-world-urbanization-prospects.html
University of Maryland, Center for Disaster Resilience, Texas A&M University, Galveston Campus, Center for Texas Beaches and Shores (UM CDR and TAMU CTBS). (2018). *The Growing Threat of Urbna Flooding: A National Challenge.* College Park: A. James Clark School of Engineering.
USACE Baltimore District. (2020). *Evaluation of Ellicott City Flood Risk Management Strategies.* Planning Division, Baltimore.
USGCRP. (2017). *Climate Science Special Report: Fourth National Climate Assessment, Volume I.* Washington, D.C.: U.S. Global Change Research Program.
Wieczorek, M. E. (2014, 07 10). Area- and Depth-Weighted Averages of Selected SSURGO Variables for the Conterminous United States and District of Columbia. United States Geological Survey. Retrieved March 2020, from https://water.usgs.gov/GIS/metadata/usgswrd/XML/ds866_ssurgo_variables.xml

Appendix A: List of soil type and area in Tiber Branch watershed

Soil Symbol	Name	Hydrologic Soil Group	Area (%)
BaA	Basher fine sandy loam, 0 to 3 percent slopes, occasionally flooded	D	0.64
ChB	Clarksburg silt loam, 0 to 8 percent slopes	C	0.12
ChC	Clarksburg silt loam, 8 to 15 percent slopes	C	0.27
Co	Combs fine sandy loam	C	2.73
GbB	Gilpin silt loam, 3 to 8 percent slopes	A	0.51
GbC	Gilpin silt loam, 8 to 15 percent slopes	A	0.38
GdC	Glenelg loam, 8 to 15 percent slopes	A	0.02
GdD	Gladstone-Legore complex, 15 to 25 percent slopes, stony	A	0.08
GfB	Glenelg silt loam, 3 to 8 percent slopes	A	3.51
GfC	Glenelg-Urban land complex, 8 to 15 percent slopes	A	3.41
GgB	Glenelg channery loam, 3 to 8 percent slopes	B	1.21
GgC	Glenelg gravelly loam, 8 to 15 percent slopes	B	0.08
GhB	Glenelg-Blocktown gravelly loams, 3 to 8 percent slopes	B	3.31
GmC	Gilpin very stony-Macove very rubbly complex, 8 to 15 percent slopes	C	1.20
GnB	Glenelg-Mt. Airy-Urban land complex, 0 to 8 percent slopes	C	0.32
GoB	Glenville silt loam, 3 to 8 percent slopes	C	2.27
GuB	Glenville-Baile silt loams, 3 to 8 percent slopes	C	1.08
Ha	Hatboro-Codorus silt loams, 0 to 3 percent slopes	D	0.31
JaB	Jackland silt loam, 3 to 8 percent slopes	D	0.37
LaB	Laidig very stony loam, 0 to 8 percent slopes	C	0.10
LaC	Laidig cobbly loam, 8 to 15 percent slopes, extremely stony	C	1.30
LeB	Lehew channery fine sandy loam, 3 to 8 percent slopes	C	0.39
LeC	Lehew channery fine sandy loam, 8 to 15 percent slopes	C	2.55

LmB	Legore-Montalto silt loams, 3 to 8 percent slopes	C	4.48
LoB	Legore-Montalto-Urban land complex, 0 to 8 percent slopes	C	15.44
LoC	Legore-Montalto-Urban land complex, 8 to 15 percent slopes	C	6.94
LrD	Legore-Relay gravelly loams, 15 to 25 percent slopes, very stony	C	6.32
LrF	Legore-Relay gravelly loams, 25 to 65 percent slopes, very stony	C	3.52
MaC	Macove channery silt loam, 8 to 15 percent slopes	B	2.80
MaD	Manor loam, 15 to 25 percent slopes	B	0.65
McC	Manor loam, 8 to 15 percent slopes	B	0.78
MgD	Monongahela silt loam, 15 to 25 percent slopes	B	6.29
MgF	Manor-Bannertown sandy loams, 25 to 65 percent slopes, rocky	B	5.07
MoB	Monongahela-Urban land complex, 0 to 8 percent slopes	C	0.39
MoC	Monongahela-Urban land complex, 8 to 15 percent slopes	C	0.44
SaB	Sassafras loam, 2 to 5 percent slopes	B	0.08
SrD	Sassafras and Croom soils, 10 to 15 percent slopes	B	1.02
UaF	Udorthents, highway, 0 to 65 percent slopes	D	5.80
UbF	Udorthents, flyash, 0 to 65 percent slopes	D	1.50
UcB	Ungers, Calvin, and Lehew channery loams, 0 to 10 percent slopes	C	0.47
UuB	Udorthents-Urban land complex, 0 to 8 percent slopes	D	4.76
W	Water	D	0.01
WaB	Walkersville silt loam, 3 to 8 percent slopes	D	7.07

Appendix B: Delineating subcatchments using GIS tools

Layers needed:

- DEM
- Stormwater catch-basins, culverts, and outfalls as point features
- Stream as a line feature

Steps to Burn Stream into DEM layer.

1. Check location of streams to ensure that the centerline matches the DEM. Creating contours for this step will help locate where the stream should be. Stream may also need to be edit to include crossing culverts.
    a. Load culvert point features.
    b. Manually draw streams
        i. Start editing and choose the streams layer
        ii. Add additional streams over areas where there are culverts and it crosses the road
2. Burn Streams into the DEM to ensure it is picked up by Flow Accumulation
    a. Conversion > To Raster > Polyline to Raster
        i. Cell size > same size as DEM layer
        ii. Environments >Processing Extent > Snap Raster > DEM layer
        iii. Environments > Processing Extent > Extent > same as DEM Layer
3. Give all values in the stream raster a depth that will create tunnels in the DEM (32.81 feet/10 meters)
    a. Spatial Analysis > Map Algebra > Raster Calculator
    b. Con(IsNull("allstreamsr"),0,*depth*)
4. Burn the stream raster into the DEM.
    a. Raster Calculator
        i. DEM Layer – stream raster (output from step 3)
5. Check different Lidar rasters
    a. Run fill on burn
        i. Spatial Analyst>Hydrology>Fill
    b. Use raster calculator to check that burned worked over culvert
        i. Raster calculator
            1. Input: burnfill-burn
    c. If output is correct and culverts are fixed continue, if not repeat process to remove them all.
6. Complete Flow Direction on Burned DEM
7. Complete Flow Accumulation on Filled Burned DEM
    a. Check flow accumulation for accuracy
8. Create subcatchments
    a. Spatial Analyst → Hydrology → Snap Pour Points
        i. Stormwater inlets are considered outlets for subcatchments in SWMM. Select inlet layer as the output for snap pour points.

ii. Select appropriate snap distance for inlets to snap to flow accumulation
    1. Inlets spatial location may be on the sidewalk and not on the road where gutter flow is accumulating. This step bringing the inlet to the flow.

b. Spatial Analyst → Hydrology →Watershed
    i. Inputs are flow direction and snapped pour points
    ii. Output: subwatershed for each snapped pour point
        1. Once completed, open Symbology→ Unique Values→ Add All Values
            a. Changes each subwatershed to a different color
        2. Check with contours to ensure accuracy

Appendix C: Analyzing stormwater ponds to get storage curves for SWMM

Stormwater management detention ponds are widely used to maintain water quality and acts as storage for stormwater under various conditions. SWM ponds are modeled as storage objects in SWMM and a storage curve is required for the depth-area relationship of the pond. SWMM uses the trapezoidal rule to compute the volume of water in the pond at any depth. These instructions were used to find the surface area-depth relationship using GIS tools.

Materials Needed:

- Digital elevation model (DEM) of the study area
- ArcMap's 3D Analyst toolbar

There are many ways to locate SWM ponds within a watershed. The ponds in the TBW were identified using the interactive map or as-built plans, but if all location were not none, the next steps were used to identify the remaining ponds and confirm known locations of the ponds. Aerial imagery was very useful in this step to confirm depressions were actually ponds.

1. Loaded the DEM into a blank map and ran the Fill test on the DEM to remove sinks from the data.
2. Using Raster Math, I divided the original DEM with the Filled DEM. This created an output that displays depression in the DEM
    a. Under symbology, I changed the classified to quantiles and made the color for first two breaks null. This allows the ponds to stand out more.

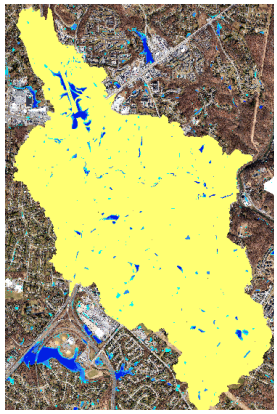

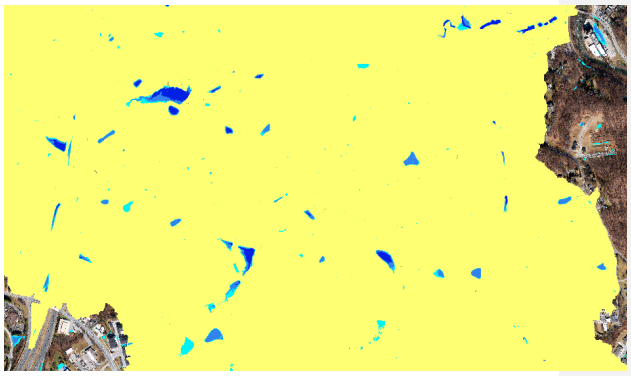

Now that each location is known, the following steps were used to gather area-depth information.

3. Create contours using the DEM to aid in finding pond boundaries.
4. Create a polygon feature class and select the polygon for editing.

a. In the *Create Features* tab, select the newly created polygon feature class and using construction tools select Auto Complete Freehand.
b. Using the contours, DEM, or aerial imagery, trace the ponds boundaries and double click to close polygon.
c. Save edits and stop editing.

5. Using the Extract by Mask tool under Spatial Analyst Tools, input the DEM and the newly edited polygon feature class.
    d. The output is the pond's elevation, check to make sure it is just the pond
    e. May have to redo step 3 to add more of the pond or remove surrounding areas.
6. The Area and Volume Statistics tool was used from the 3D Analyst toolbar to calculate the surface area for various depths

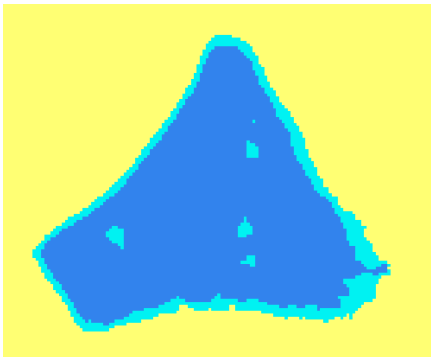

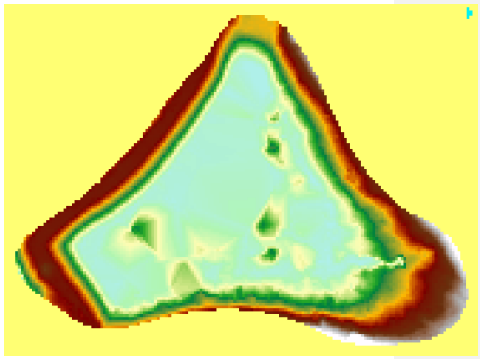

The above steps 3-6 are detailed below for more assistance.

1. Open the toolbox and click on Data Management
    a. Click on feature class
        i. Choose an appropriate folder to save the feature class in and name the feature something related to the area.
        ii. Keep as output as a polygon.
        iii. Select coordinate system.
        iv. Save
2. Next, edit the feature class so that it is the area of the pond
    a. Open the editor toolbar
        i. If the editor window doesn't open, click on editor in the toolbar and select "Editor Window" → Create Features
    b. Click on editor and then "Start Editing"
    c. In the editor window, select the shape of the polygon (ex. Auto Complete Freehand) and begin drawing it on the map
        i. Be sure to get as close to the pond as possible.
    d. Click on editor and then "Save edits" and then Stop editing.
3. To clip the feature class with the DEM.

a. Open the toolbar.
    i. Click on Spatial Analysis
    ii. Extraction→ Extract by Mask
b. Select the inputs and name the output
    i. Inputs are the DEM and the output from extraction.

4. Add the "Area and Volume" tool to the 3D Analyst Toolbar.
    a. Launch the 3D Analyst Toolbar In the toolbar header, pull down the small arrow to "Customize". Click Customize.
    b. In the dialog box that appears, choose the tab "Commands".
    c. In the right-hand menu, find the item "Area and Volume". Click and drag this item to the **3D Analyst Toolbar**. Close the dialog box (not the toolbar). Click *"Area and Volume"* in the 3D Analyst Toolbar to launch the tool.
        i. The input surface is the output from step 3.
        ii. Height of plane is adjusted for different heights that surface area is needed
            1. Starting from the minimum and to maximum of pond
        iii. Calculate statistics *below* plane is selected.
        iv. Surface area is provided for each depth entered and can be saved in a text file for future retrieval.